



MIDDLE EAST TECHNICAL UNIVERSITY

ELECTRICAL & ELECTRONICS ENGINEERING DEPARTMENT

EE464

Static Power Conversion-II

TERM PROJECT

"DC/DC Converter Design for Tesla Model S"

Student Names	–	Student ID's
Ceyhun Koç	-	2166833
Enes Canbolat	–	2231546
Eren Özkara	-	2232551

Table of Contents

1. Introduction.....	2
2. Topology Selection	2
3. Operating Mode Selection	3
4. Analytical Calculations and Simulation.....	3
5. Magnetic Design	6
6.1. Controller.....	11
6.2. Discrete Component Selection	13
7. Detailed Simulation Results.....	15
8. Loss Calculations	22
9. Thermal Calculations	26
9.1. MOSFET	27
9.2. Diode	27
10. Hardware Design.....	28
10.1. Schematic Design.....	28
10.2. PCB Design.....	31
11. Cost Analysis.....	41
12. Conclusion.....	43
References	44

1. Introduction

Nowadays, electric vehicle technology is a rising trend and Tesla is leading this technological leap. In Tesla Model S, there are two batteries, high and low-voltage ones, and there is a connection between them. The problem is that their voltage levels are so different, and it is needed to design a converter between them. At this point, Martian Power Solutions introduce a solution for this problem. Specs of the project are listed below, and the rest of the report contains the topology selection, some theoretical calculations, the component selection including the magnetic core design step and the realistic simulation results are mentioned in detail. Also, a schematic of the design is shown that will be used in the PCB design process.

- **Minimum Input Voltage:** 220 V
- **Maximum Input Voltage:** 400 V
- **Output Voltage:** 12 V
- **Output Power:** 100 W
- **Output Voltage Peak-to-Peak Ripple:** 4%
- **Line Regulation** (Deviation of percent output voltage when the input voltage is changed from its minimum to maximum or vice versa): 3%
- **Load Regulation** (Deviation of percent output voltage when the load current is changed from 10% to 100% or vice versa): 3%

Thanks to this project, we as engineers of Martian Power Solutions will improve our engineering skills. Moreover, we have a chance to use the theoretical knowledge that we have learned in the EE464 course.

2. Topology Selection

In the scope of this project, three main topologies come forward that are Flyback converters, Forward converters, and Push-Pull converters. All these topologies can be used between the high and low-voltage batteries of the Tesla Model S with an isolation mechanism. Also, all of these converter topologies give chance to adjust the output voltage with another parameter, the turns ratio. Flyback Converter topology is created from the buck-boost converter topology with a transformer that helps to store the energy. The Flyback is the most common and most studied topology. Therefore, there are lots of source and application notes for this choice. Although it is preferable for low-power applications, the topology can supply the output current up to 10 A safely which is lower than the given specs of the project. The forward converter is created from the buck converter topology with a transformer. Like Flyback, Forward Converters are preferable for low-power applications. In the magnetic design, a gapless core can be used for the Forward Converter design and this increases the L_m value which means less ripple at the output; however, due to extra inductor and diode cost could be higher than the Flyback converter. Also, in DCM mode gain changes dramatically. Moreover, MOSFET should withstand higher voltages which increases the size of the design. Forward Converters work stable even the exceeding 15 Amperes limit. Due to these crucial disadvantages, Forward Converter is not the selected topology. Push-Pull Converter is a kind of Forward Converter with two primary windings to create a dual-drive winding. Utilization of the magnetic core is better compared to the two other topologies since in this topology the magnetic core can operate both the 1st and 3rd quadrants of the B-H curve. On the other hand, the switching control mechanism

is harder than the other ones because as known both switches never should be activated at the same time. Moreover, Push-Pull Converters are a better choice for very high-power applications. Considering the above criteria Flyback Converter topology is the best choice for this project. Furthermore, the engineers of Martian Power Solutions had some experience in designing Flyback Converter circuits and using these experiences results in a better solution for this project.

3. Operating Mode Selection

There are both advantages and disadvantages of the two operating modes, CCM and DCM. CCM is preferable for high-power applications while DCM is preferable for low-power applications. The switching performance of DCM is better since the diode operates zero current just before the activating time. Also, the transformer size in this mode is smaller; however, the peak and RMS value of the output current is higher than the CCM operation. This situation increases the stress level on the output capacitor and conduction losses on the MOSFET. Therefore, for the cases where the output has high voltage and low current DCM is a better option. On the other hand, CCM should be a better selection for the low output voltage and high output current. Furthermore, the controller is another important decision criterion of operating mode. Due to the specs of the project, there are no many suitable controllers or PWM generator selections in the market. LT8316 was chosen as a controller of this project and why this controller was selected is explained in the "Controller Selection" section in detail. In the description of the controller, it can be seen that the IC has a pin called the DCM pin. This pin detects the change of the voltage with respect to the time (dV/dt) of the switching waveform and controls the operating mode by adjusting the duty cycle of the system. The aim of this control mechanism called critical conduction mode is to operate the circuit almost in the boundary conditions since the controller improves load regulation without extra resistors and capacitors at the output side and reduces the transformer size with high efficiency at the boundary conditions. In short, the Flyback Controller with LT8316 operates at the boundary between the continuous and discontinuous conduction modes. To keep the operation at the boundary, the switching frequency of the system is variable. Thanks to the controller, the advantages of both continuous and discontinuous modes can be enjoyed in the design.

4. Analytical Calculations and Simulation

This section contains analytical calculations and simulations for flyback converters. Since the controllers, whose details will be explained later, force the system to operate in boundary mode, calculations will be made according to the continuous current mode, and values of components will be taken in accordance with boundary mode.

Duty cycle values close to ideal conditions are calculated as in Equation 1. As a result of the research of the controller and transformer design, it was decided that the turn ratio value should be close to 4. Under normal conditions, considering the power loss and thermal conditions, the transformer ratio should be adjusted so that the duty cycle is optimally 0.5. However, due to the working mechanism of the controller selected in accordance with the project, the system will operate at a low duty cycle.

$V_{out} = V_{in} \left(\frac{D}{1-D} \right) \left(\frac{N_2}{N_1} \right)$	(1)
$V_{in} = 220\text{ V}, D = 0.18; V_{in} = 400\text{ V}, D = 0.11$	(2)

The minimum required inductance value for Continuous Current Mode depends on the frequency. The controller works with around 100kHz at input voltage values. The worst-case has been taken into consideration in the calculations.

$L_{Mmin} = \left(\frac{(1-D)^2 R}{2f} \right) \left(\frac{N_1}{N_2} \right)^2$	(3)
$f = 100\text{ kHz}, L_{Mmin} = 91.25\mu\text{ H}$	(4)

When the switch is off, the voltage falling on the switch is calculated in equation 5.

$V_{sw_open} = V_{in} + V_{out} * N, V_{sw_max} = 448\text{ V}$	(5)
---	-----

The output voltage limit suitable for the project purpose is calculated according to the 7 and 8 equations. The worst-case has been taken into consideration in the calculations.

$\Delta V_o = \frac{\Delta Q}{C} = \frac{V_o * D * T_s}{R * C}, \quad \frac{\Delta V_o}{V_o} \leq 0.04, \quad C \geq 31.25\text{ }\mu\text{F}$	(7)
$\Delta V_{o,ESR} = I_{LM,max} * \left(\frac{N_1}{N_2} \right) * r_c, \quad r_c < 0.006\text{ ohm}$	(8)

These calculated values are symbolic. It depends on the choice of components used and the mode in which the controller is operating. Therefore, after simulations with the controller, different calculations can be made using the same equations.

A converter diagram was created with MATLAB-SIMULINK to test analytical calculations the diagram can be seen in the following Figure 1. In the model, the circuit elements are taken as the values in the analytical calculation.

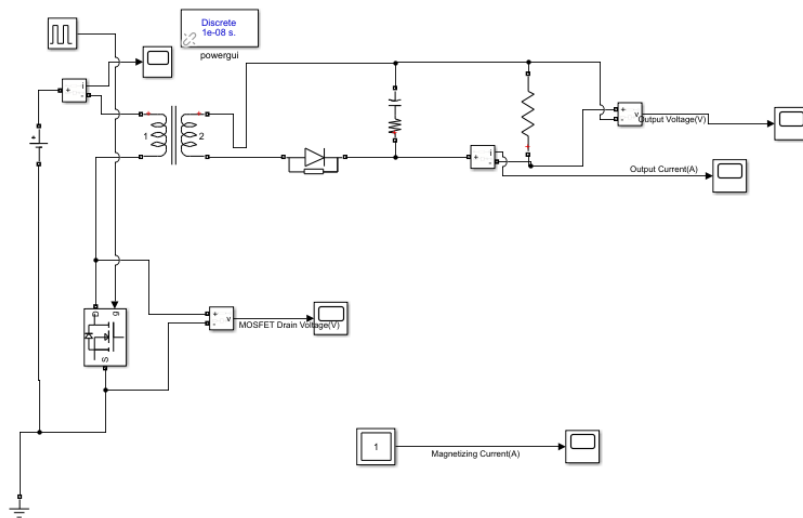


Figure 1 Flyback Converter Simulink Model

While selecting the capacitor value, the ESR value of the capacitor was also considered. The output voltage ripple value is approximate to what was expected. The output voltage waveform can be seen in the following Figure 2.

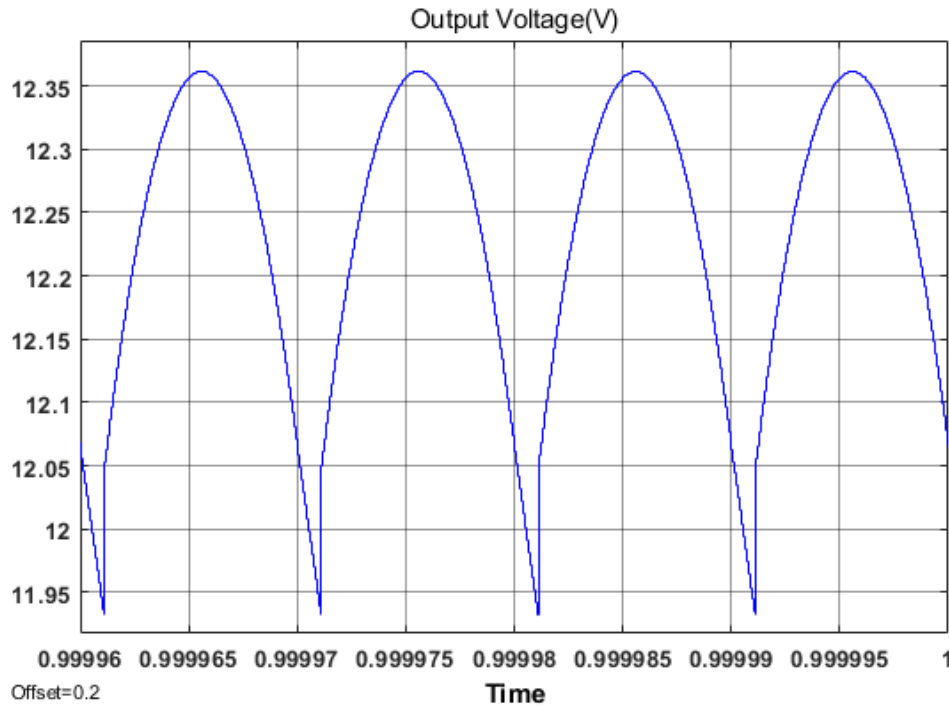


Figure 2 Output Voltage Waveform

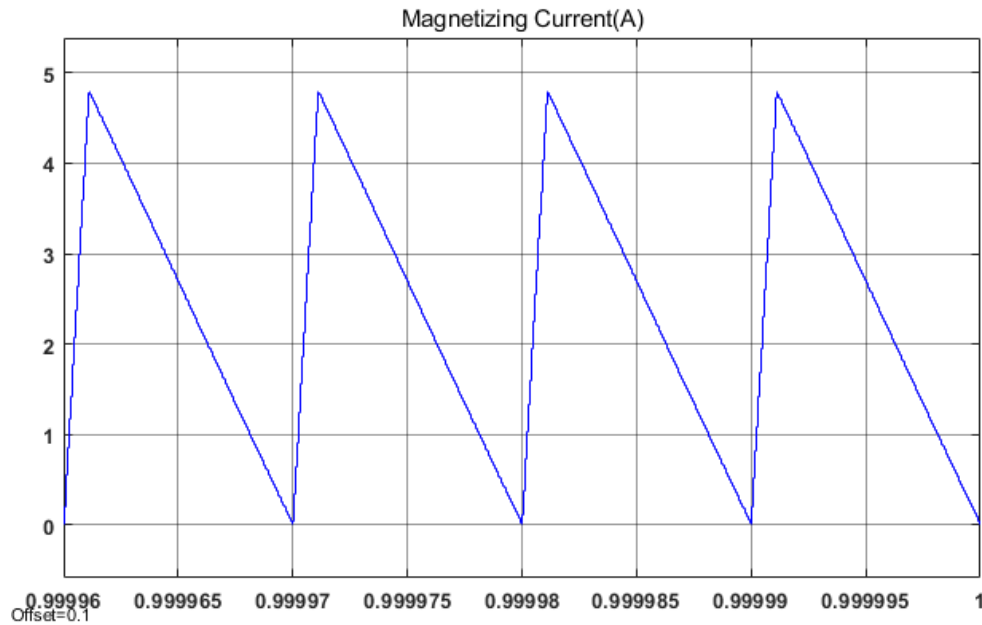


Figure 3 Magnetizing Current Waveform

As can be realized that the converter works in boundary mode from the magnetizing current in Figure 3. Furthermore, the voltage waveform of the MOSFET is shown in the following Figure 4.

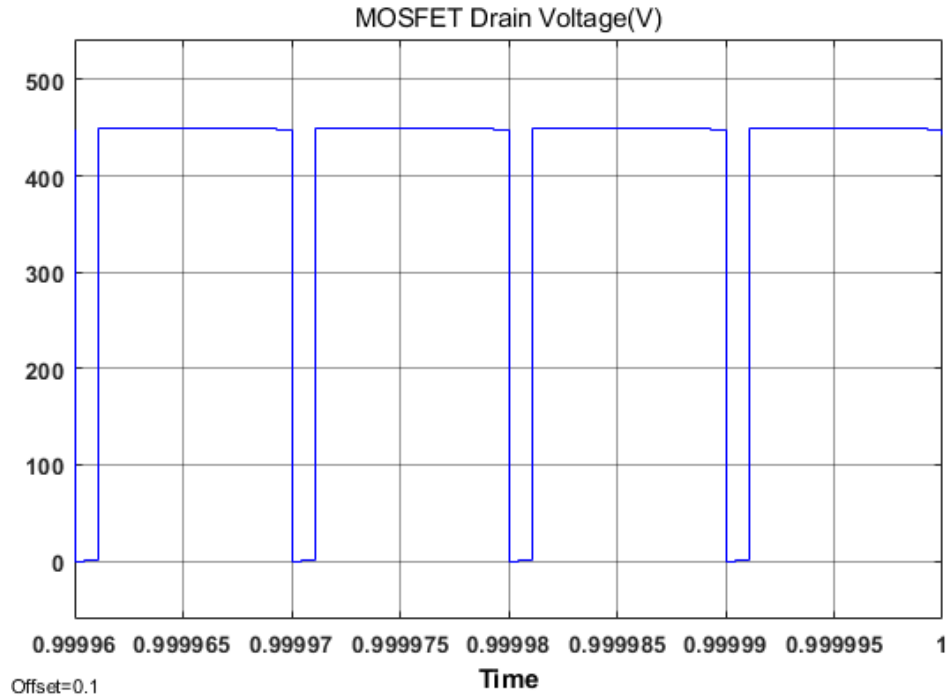


Figure 4 MOSFET Drain Voltage

The breakdown voltage falling on the MOSFET while in off mode is also seen in Figure 4. The result is the same as the analytical model. This value should also be considered while choosing the MOSFET.

Analytical calculations and simulations made so far are the first steps of the project. In later stages, these analytical equations were used iteratively. However, the controller directly affects the converter's duty cycle and frequency. Therefore, it is compulsory to make a detailed simulation with the controller after the component selection. Components are selected iteratively according to the results of the simulations.

5. Magnetic Design

Since the controller to be used will receive the power supply over transformer winding, a transformer with three windings will be designed. The transformer schematic can be seen in Figure 5.

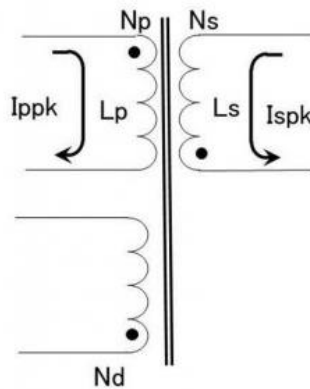


Figure 5 Transformer Schematic

Considering the size of the transformer to be designed, the duty cycle should be less than 0.5. As the duty cycle increases the size of the transformer should increase as the energy to be stored increases. The flyback reflected output voltage (VOR) is equal to the secondary output voltage plus the secondary diode on voltage (VO) multiplied by the transformer winding ratio (N_p/N_s). Flyback reflected output voltage indicates the winding ratio and the duty cycle ratio (D). Diode forward voltage is assumed to be 1 V in calculations. Moreover, In the iterative calculations, it was decided that the winding ratio should be 26/6.

$VO = V_{out} + V_F, \quad VO = 12 + 1 = 13 \text{ V}$	(9)
$VOR = VO * \frac{N_p}{N_s}, \quad VOR = 13 * \frac{26}{6} = 56.333 \text{ V}$	(10)
$D_{max} = \frac{VOR}{(V_{in_min} + VOR)}, \quad D_{max} = 0.204$	(11)

The minimum input voltage value to be used in the project is 220V, so the maximum duty cycle value has been calculated accordingly. Also, the sum of the input voltage value and the reflected output voltage value indicates the maximum breakdown voltage that will fall on the switch.

Then, the secondary winding inductance (L_s) value and the secondary-side peak current (I_{spk}) value are calculated. Since the controller tries to make the converter work in boundary mode, the calculations are made according to discontinuous mode (The worst case). The most critical point in this calculation is the point where the output current is maximum, so the calculations are made accordingly.

$I_{out_{max}} = \frac{P_{out}}{V_{out}}, \quad I_{out_{max}} = 8.333 \text{ A}$	(12)
$L_s = \frac{(V_{out} + V_F) * (1 - D_{max})^2}{2 * I_{out_{max}} * f_{sw_{max}}}, \quad L_s \leq 4.9 \mu H, \quad L_s = 4.34 \mu H$	(13)
$I_{spk} = \frac{2 * I_{out_{max}}}{1 - D_{max}} = 20.1 \text{ A}$	(14)

In simulations made with the controller, it was determined that the maximum frequency used by the controller was 100kHz, so the calculations were made by taking the maximum frequency of 100kHz. For the converter to work in boundary mode, the inductance value must be close to or smaller than the calculated value.

$L_p = L_s * \left(\frac{N_p}{N_s}\right)^2 = 81.5 \mu H$	(15)
$I_{ppk} = \frac{I_{spk}}{N_p/N_s} = 4.83 \text{ A}$	(16)

Primary winding inductance (L_p) and the primary peak current (I_{ppk}) were calculated using the winding ratio from the calculations made for the secondary side.

After these calculations, the size of the transformer and the magnetic material to be used were decided. PC47EI25 was decided to be used as a result of the iterative calculations made by also looking at the fill factor. The size of the EI25 core is sufficient for the project and the PC47 ferrite core whose properties can be seen in the following Table 1 used are also suitable for the project purpose.

Table 1 Magnetic Properties of the PC47EI25

	Effective cross-sectional area Ae (mm ²)	Maximum Magnetic Flux density (T)	AL-value with the air gap (nH/N ²)
PC47EI25	41	0.42	125

By using an air-gapped ferrite core, the transformer cost was kept low, and it provided an advantage in size. Using these properties of the transformer, primary winding turns (N_p) can be calculated. The primary winding turns must be adjusted so that the core cannot be in saturation during operation (Equation 17). L_p value can be designed with AL-Value and N_p (Equation 18). Also, the maximum MMF value in the core can be calculated with equation 19. After calculating the primary winding turns, the secondary winding number can be calculated using the winding ratio (Equation 20). In addition, since the input voltage is equal to the output voltage in the controller, the number of winding turns must be equal (Equation 21).

$N_p = \frac{V_{in} * D * T_s}{A_e * B_{sat}} = L_p * \frac{I_{ppk}}{A_e * B_{sat}} = 22.8, \quad N_p \geq 22.8$	(17)
$N_p = \sqrt{\frac{L_p}{AL}} = 25.53, \quad N_p = 25$	(18)
$MMF = \frac{N_p}{N_s} * I_{ppk} = 120 \text{ A.t}$	(19)
$N_s = \frac{\frac{N_p}{N_p}}{N_s} = 6$	(20)
$Nd = 6$	(21)

Finally, physical dimensions of the transformer core and cables to be used are needed to make fill factor calculations. Core dimension values are taken from the datasheet. Core dimensions and properties can be seen in Table 2, Figure 6, and Table 3, respectively. While choosing the cable, attention has been paid to ensure that the current value that the cable can carry is higher than the maximum current value.

Table 2 Core Dimensions

Core	A (mm)	C(mm)	D (mm)	E(mm)	F (mm)
EI25	25.3	5.75	6.5	19	12.35

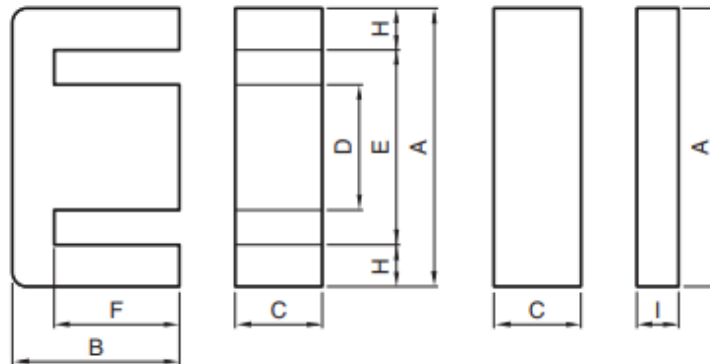


Figure 6 Core Dimensions

Table 3 Cable Properties

Wire	Area (mm ²)	Diameter(mm)	Ampacity (75°C)	Resistivity (p) (10 ⁻⁸ Ω.m)	Absolute magnetic permeability(u) (10 ⁻⁷ H/m)
AWG10	5.26	2.588	35	1.678	12.55
AWG20	0.518	0.812	11	1.678	12.55
AWG30	0.509	0.255	0.86	1.678	12.55

Using these dimensions, the fill factor is calculated as in Equations 22, 23, and 24.

$Window_A = \frac{A - D}{2} * (F + 1mm) = 116.1 \text{ mm}^2$	(22)
$Cable_A = AWG20 * Np + AWG10 * Ns + AWG30 * Nd = 48 \text{ mm}^2$	(23)
$Fill_{Factor} = \frac{Cable_A}{Window_A} = 0.41$	(24)

Furthermore, the distribution of current in a conductor is almost uniform when the system is DC. However, the current in the transformer behaves as an AC current even though the converter is a DC/DC converter. Current flows in a transformer conductor are not uniform, therefore, the skin effect should be taken into consideration while choosing cable. Since skin depth dictates effective cross-section area, it is significant while calculating the AC resistance of the cables. The resistance values are calculated according to the following equations and as it is seen that the cable used AWG20 reaches the highest AC resistance value, the values of the AWG20 cable are calculated as an example. While making these calculations, the values in Table 2 and Table 3 were used.

$length = \left(C + \frac{D + E}{2}\right) * 2, \quad AWG20_{length} = length * Np = 0.962 \text{ m}$	(25)
$Skin_{depth} = \sqrt{\left(\frac{p}{\pi * f * u}\right)} = 207 \mu m$	(26)
$Effective_{Area} = Skin_{depth} * \pi * Diameter,$ $A_{eff_{AWG20}} = Skin_{depth} * \pi * AWG20_d = 0.528 \text{ mm}^2$	(27)
$R_{AC} = p * \frac{length}{Effective_{Area}}, \quad R_{AC20} = p * \frac{AWG20_{length}}{A_{eff_{AWG20}}} = 30 \text{ m}\Omega$	(28)

The resistance values of AWG 10, AWG 20, and AWG 30 cables are 2, 30, and 22 mΩ, respectively, so they can be neglected. With calculated values, copper losses due to transformer wiring will be around 2 W. This calculation does not include the proximity effect; therefore, it should be more. Moreover, we want to design a more compact and less lossy winding design therefore we will use Litz wire.

For the 50-100kHz range, AWG38 Litz wire is suitable, and we can construct AWG10, AWG20, and AWG30 wires from AWG38. The following Figure 7 shows the Litz wire constructions.

Round Litz										
Equivalent Gauge	Circular Mil Area	Number of Strands	Strand Gauge	Film Coating 1	Construction Type	Outer Insulation 2	Nominal Outside Diameter (inches)	Nominal Lbs./MFT.	Direct Current Resistance OHMS/MFT.	Construction
Recommended Operating Frequency – 50 KHZ to 100 KHZ										
30	112	7	38	S	1	SN	.017	.382	98.9	7/38
28	160	10	38	S	1	SN	.020	.538	69.3	10/38
26	256	16	38	S	1	SN	.024	.849	43.3	16/38
24	400	25	38	S	1	SN	.029	1.31	27.7	25/38
22	640	40	38	S	1	SN	.036	2.08	17.4	40/38
20	1,056	66	38	S	1	SN	.050	3.50	10.8	3/22/38
18	1,600	100	38	S	2	SN	.061	5.27	7.10	5x20/38
16	2,592	162	38	S	2	SN	.073	8.50	4.38	3/54/38
14	4,160	260	38	S	2	SN	.093	13.6	2.73	5x52/38
12	6,720	420	38	S	2	SN	.118	22.5	1.73	5x3/28/38
10	10,560	660	38	S	2	DN	.150	35.9	1.11	5x3/44/38
8	16,800	1,050	38	S	2	DN	.189	57.0	.692	5x5x42/38
6	26,400	1,650	38	S	2	DN	.236	89.4	.440	5x5x66/38
4	42,000	2,625	38	S	2	DN	.296	146.	.283	5x5x3/35/38
2	66,240	4,140	38	S	5	SNB	.494	247.	.180	6(5x3/46/38)
1	84,000	5,250	38	S	5	SNB	.551	311.	.141	6(5x5x35/38)
1/0	105,600	6,600	38	S	5	SNB	.613	389.	.112	6(5x5x44/38)
2/0	136,000	8,500	38	S	5	SNB	.749	522.	.087	10(5x5x34/38)
3/0	168,000	10,500	38	S	5	SNB	.828	642.	.070	10(5x5x42/38)
4/0	211,200	13,200	38	S	5	SNB	.966	824.	.056	12(5x5x44/38)

Figure 7 Litz Wire Construction

$R_{dc} = \frac{RS * ((1.02)^{Nb}) * ((1.03)^{Nc})}{Ns}$	(29)
$R_{dc}(AWG10) = 3.7 \text{ m}\Omega/\text{m},$ $R_{dc}(AWG20) = 36 \text{ m}\Omega/\text{m}, R_{dc}(AWG30) = 330 \text{ m}\Omega/\text{m}$	(30)
$R_{AC10} = 0.8 \text{ m}\Omega, \quad R_{AC20} = 34.6 \text{ m}\Omega, \quad R_{AC30} = 73.1 \text{ m}\Omega$	(31)

In Litz wire, the resistance calculation formula can be seen in Equation 29. Nb is the number of bunching operations, Nc is the number of cabling operations and Ns is the number of individual strands in this formula. While calculating the resistance value for each cable winding, the previously calculated mean length turn was used. Since both skin effect and proximity effect are eliminated in the Litz wire structure, it can be considered that AC resistance equal to DC resistance. Resistance values for each cabling can be seen in Equation 30.

One of the important points of magnetic core selection is that the core must provide sufficient inductance values despite the decreasing AL value with DC-Bias. In Equation 19, the maximum MMF value is calculated with the maximum current value on the core, and when the datasheet of the core material is examined, it was observed that the core did not deviate from the axis in the graph at calculated MMF value as seen in Figure 8. Also, the minimum number of turns required to avoid saturation is calculated in Equation 17.

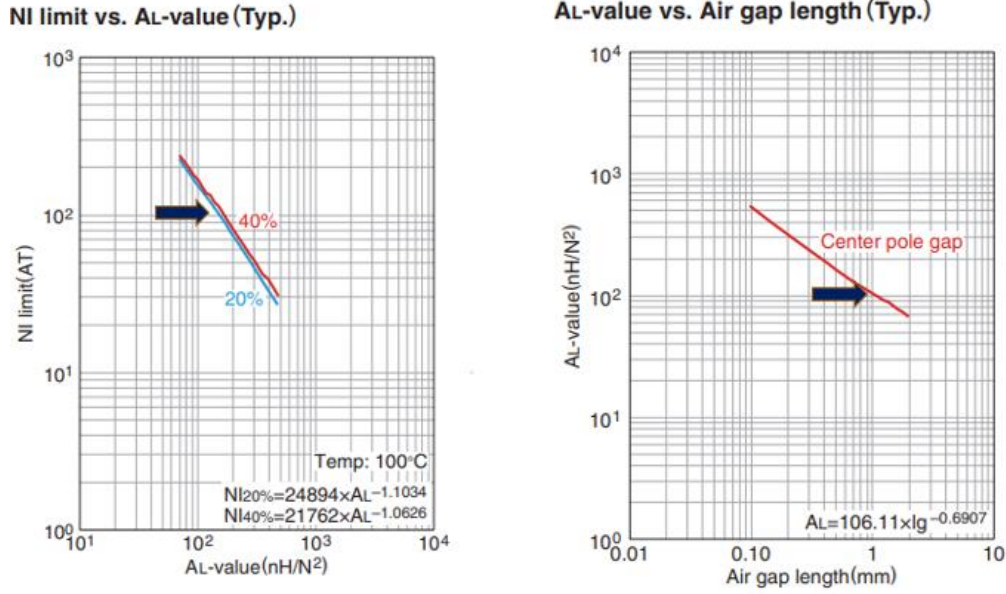


Figure 8 NI limit and Air gap vs AL value Graphs

Since the transformer transfers the stored energy in the Flyback Converter design, a certain amount of air gap should be left in the core design. The 1 mm air gap will cause the AL value used for the design as shown in the above Figure 8.

$V_{p_{rms}} * I_{p_{rms}} = \frac{N_p * A_e * B_{sat}}{D * T_s} * I_{p_{rms}} = P_o = 197.5 \text{ W}$	(32)
$V_{p_{rms}} * I_{p_{rms}} = 100 \text{ W} = \frac{N_p * A_e * B_{operating}}{D * T_s} * I_{p_{rms}}, \quad B_{operating} = 0.2 \text{ T}$	(33)

As stated before, the core used in the design is saturated at 0.42 T. When Faraday's law is used, the transformer can provide 197.5 W power with saturation flux density value (Equation 32). Again, using Faraday's law, the average operating flux density value can be calculated (Equation 33). It is noted that there will be a ripple in the flux density value during the operation without saturation.

6. Component Selection and Controller

In this part of the report, selected components, purposes and outcomes will be discussed. Basically, to design a system with an analog controller, we firstly selected the controller and then arranged other components, such as transformer design, output capacitor selection, output diode selection, switch selection, etc.

In this final report, we will review the selected components, moreover, we will discuss the changed components compared with the Simulation Report. If we make an overview, the output diode, D-Z snubber, and connectors have changed. Moreover, to protect our board and output from high voltages, we have placed a TVS diode into our project.

6.1. Controller

While selecting the controller, the main aim was to have a wide input voltage range(220V-400V) and to operate at 100W operation. To simulate the closed-loop design easily, products

of Analog Devices have been investigated. In these ranges, we have ended up with LT8316 and LT3752 controllers; however, LT3752 is an active clamp forward controller and accepts only 100V input maximum, however when LT8316 is examined, it has a wide operating input voltage range from 16V to 600V, and datasheet specifies that the controller can operate up to 100W. And when we investigate the configuration, the switch is connected externally, and the controller is operated by taking output voltage and current as feedback, which means if we arrange these external components for 100W operation, we could easily use that controller. So, we have decided to use LT8316 as the controller.

The main advantage of LT8316 is, the voltage feedback of the output voltage is taken from a tertiary winding, which means that in closed-loop control we do not need any optocoupler or other kind of isolation, which is a cost-effective solution. Moreover, we will only place the third winding into the transformer core with a very thin cable due to the high impedance of sense pins, so we will save space compared with the optocoupler isolation case. In addition, optocouplers are very sensitive components, and generally, they need a 3.3V or 5V supply; however, we do not need any power IC, thanks to tertiary winding. The feedback resistor selection will be discussed in the feedback resistor part. We are able to use the tertiary winding as a solution of LT8316, which is a boundary mode operation. In this mode, the output voltage is sampled from the tertiary winding, when the secondary current is almost zero. The falling voltage is detected by the DCM pin by sensing dV/dT and sampled from the FB pin. With the boundary operation, the output diode voltage drops to zero in every cycle, so parasitic resistive voltage drops do not cause load regulation errors. Moreover, with the boundary operation, we can select a smaller transformer compared with CCM.

The other feature of the controller is current, so power limitation. The sense pin of the controller accepts 100mV maximum, and when the sense resistor voltage reaches that value, the controller limits the duty cycle to prevent the circuit. The sense resistor selection will be discussed in the "6.2. Discrete Component Selection" section.

In short, an example application of the selected controller LT8316 is shown in Figure 9, one can find the example application of LT8316. In this figure, all mentioned pin connections can also be seen, and this application example is a good guide for this project.

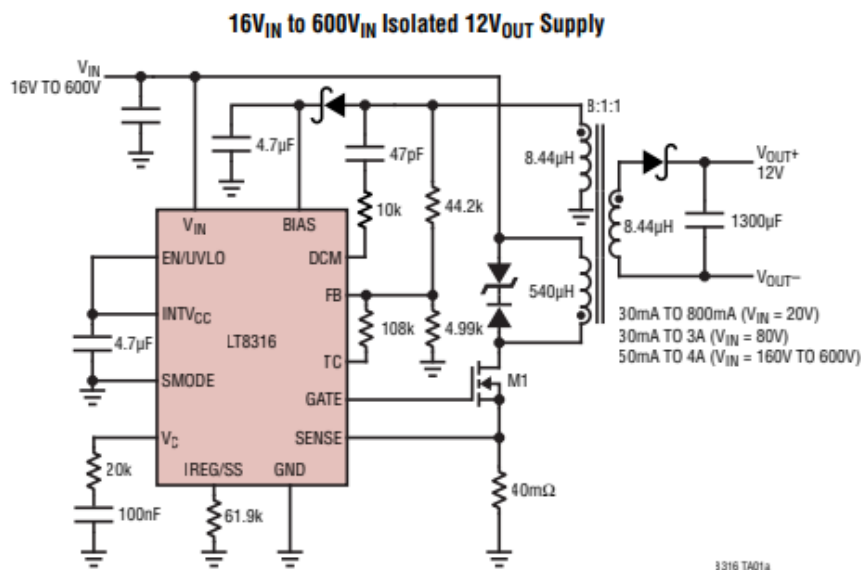


Figure 9 Typical Application of LT8316

Another safety function of the LT8316, the EN/UVLO pin. This pin is compared with 1.22V internally, so if the voltage of this pin is lower than 1.22V, the converter will not operate for safety purposes. So, in this project, we have a 220V-400V input range, and we can arrange a high impedance voltage divider for that pin so that under a critical voltage, the controller does not operate. The protector resistor selection will be discussed in the UVLO Resistor part.

6.2. Discrete Component Selection

a. Feedback Resistor Selection:

The feedback pin compares the output voltage with a 1.22V comparator, and to have a 12V output, we must divide the 12V into 1.22V; however, we have a small output, compared with the input voltage, so we need to consider the output diode forward voltage drop. The formulation in the datasheet is given as Equation 34.

$V_{out} = \left(1 + \frac{R_{FB2}}{R_{FB1}}\right) * \frac{1.22}{N_{TS}} - V_F$	(34)
--	------

In this case, the output diode has a 0.95V forward voltage drop, the output voltage is 12V, and N_{TS} , tertiary to secondary turns ratio, is 1. So that, the ratio between the feedback resistors becomes 9.6147. In this case, we can use R_{FB2} as 48.1K Ω and R_{FB1} as 5K Ω . However, when the detailed simulation is investigated, it is observed that with 47K Ω and 5K Ω resistors we obtain better output voltage. This may be a consequence of the inner reference voltage or the diode forward voltage drop. So, we will use 47K Ω and 5K Ω feedback resistors.

b. Sense Resistor Selection:

As discussed in the controller part, a proper sense resistor should be selected to set the maximum output current. LT8316 datasheet specifies the sense resistor formulation as Equation 35.

$I_{OUT(max)} = \frac{100mV}{2 * R_{SNS}} (1 - D) * N_{PS}$	(35)
---	------

When we look at the detailed simulation part, the duty cycle changes between 0.1 and 0.2, and the primary to secondary turns ratio is detected as 26:6 in magnetic design part, so we find the maximum value of sense resistor as 17.5m Ω , however, to stay in the safe zone we will select a 10m Ω sense resistor. [1] This resistor selection means that the output current will be disabled and the MOSFET will be in OFF position **after 10A current, which is an overcurrent protection.**

c. UVLO Resistor:

As specified in the controller part, the UVLO pin compares the pin voltage with 1.22V and cuts the operation below that value. The project specifies 220V-400V input voltage, so if 200V is selected as cut-off voltage, we need to divide that voltage to 1.22V. Equation 36 shows the UVLO voltage division.

$200V * \frac{R_{UV1}}{R_{UV1} + R_{UV2}} = 1.22V$	(36)
--	------

In this equation, if we select R_{UV2} as $1.5M\Omega$, we need to select R_{UV1} as $9.2K\Omega$, so we will use these values in our circuit.

d. MOSFET Selection:

As seen in the detailed simulation part, MOSFET sees 450V and 6A maximum, so we are needed to select a MOSFET for that criteria. In this manner, N-Channel MOSFET with 550V and 7.6A ratings have been selected, because as the case temperature increases, the maximum drain current decreases. The MOSFET is Infineon Technologies IPD50R500CEAUMA1. [2]

e. Output Diode Selection:

As seen in the detailed simulation part, the output diode sees a maximum 110V reverse voltage and 22A peak (8.33A average) forward current. In Simulation Report, we have selected a diode whose ratings are 170V and 30A, however, when we make thermal analysis, the temperature rise was very high. In order to stay in the safe zone and operate without any coolers, we have selected a diode with 150V reverse voltage and 3A average current, Comchip Technology CDBB3150-HF. When we make thermal analysis, by using five parallel diodes, we can use them without any coolers.

f. Tertiary Diode Selection:

The diode is placed before the BIAS pin of the controller, as can be seen in Figure 7. This diode sees the same reverse voltage as the output diode; however, the current does not exceed 100mA, so we have selected 150V, 1A Vishay ES1CHE3_A/H. The main functionality of this diode is, it is a Schottky diode, so there is not a reverse recovery instance. [4]

g. Output Capacitor Selection:

As seen in the detailed simulation part, the output capacitor has nearly 20A current ripple, so in order to stay in %4 voltage ripple criteria, the equivalent ESR must be a maximum $24m\Omega$, and the ripple current of the capacitor, specified in the datasheet, should be minimum 20A. In this manner, we have used Aluminum-Polymer capacitors because this type has a higher ripple current, and connected four of them parallel, to achieve 20A ripple, because we have selected 330uF, 16V, ripple @100kHz: 5A, ESR: $14m\Omega$ KEMET A750KK337M1CAAE014. [5] In this way, we have decreased the ESR, too.

h. RCD Snubber Selection:

As seen in Figure 7, and as seen in the datasheet, the manufacturer proposes a D-Z snubber upper side of the switch, to prevent the switch and the circuit from voltage spikes. However, when we include leakage inductance and make a simulation, the D-Z snubber could not be helped and the voltage overshoot was up to 750V, so we have determined to add RCD snubber to compensate for voltage overshoots. The resistance and capacitance voltages are determined from simulation, where the capacitor is 0.1uF 200V and the resistor is 5.6kohm and its rating is selected for worst case which is 3.5W. The diode sees nearly 400V, so the selected diode is Vishay S1J-E3/61T with 600V, 1A ratings.

i. TVS Diode

In this project, one of the bonuses is overvoltage protection. In order to protect our circuit from overvoltage cases, we have placed a TVS diode between input and ground. In this way,

As the project specs indicate that the input voltage can vary between 220V and 400V. The input voltage changing with respect to time is shown in Figure 11. Also, Figures 12 and 13 show that the performance of the output voltage and the output voltage ripple, respectively.

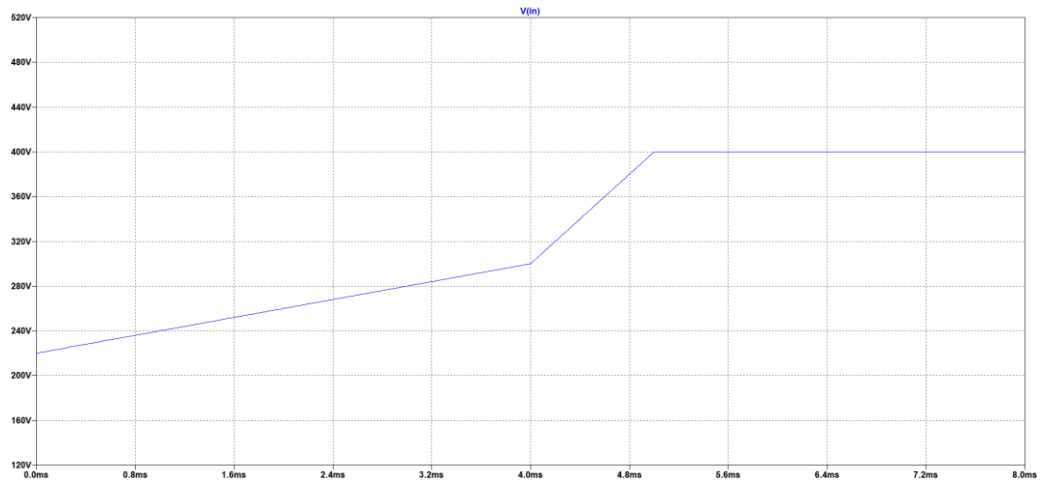


Figure 11 Varying Input Voltage

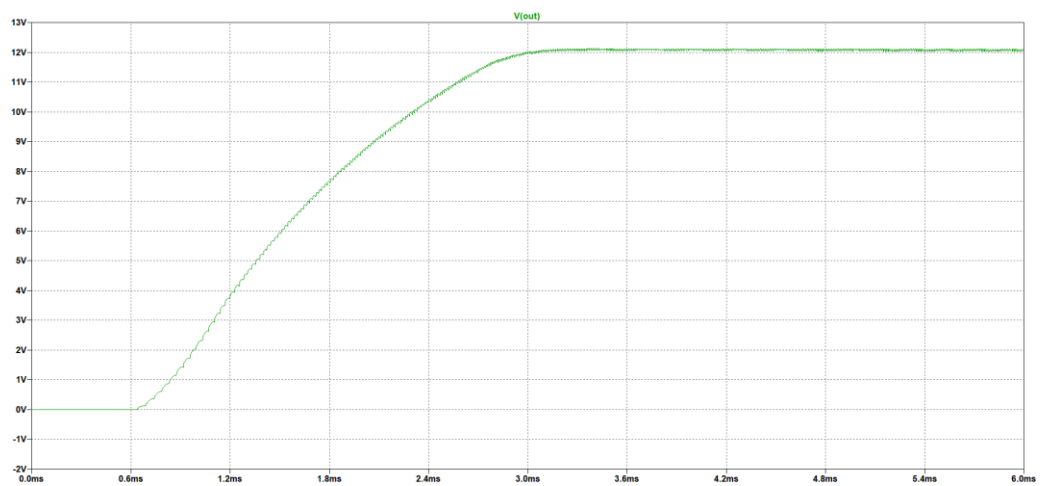


Figure 12 Output Voltage Performance for Varying Input Voltage

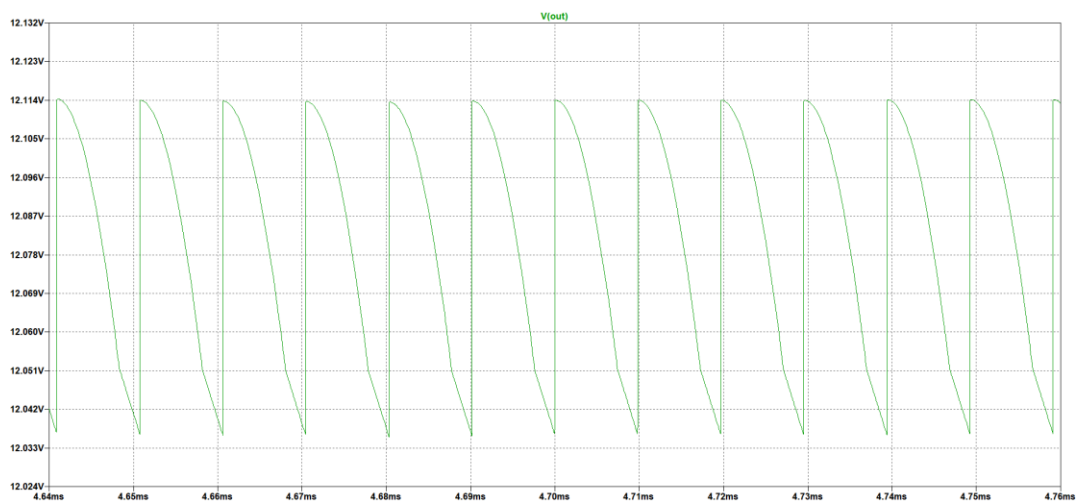


Figure 13 Output Voltage Ripple for Varying Input Voltage

As can be seen in the above figures, the output voltage almost is not affected by the varying input voltage. It can give 12V with a small ripple which is in the specified ripple margin.

The following Figure 14 shows the output voltage performance. As can be seen in that figure, the controller has a soft start property and the output voltage reaches 12V around 145ms. Since the output voltage reaches 12V almost the same time even for the extreme cases,

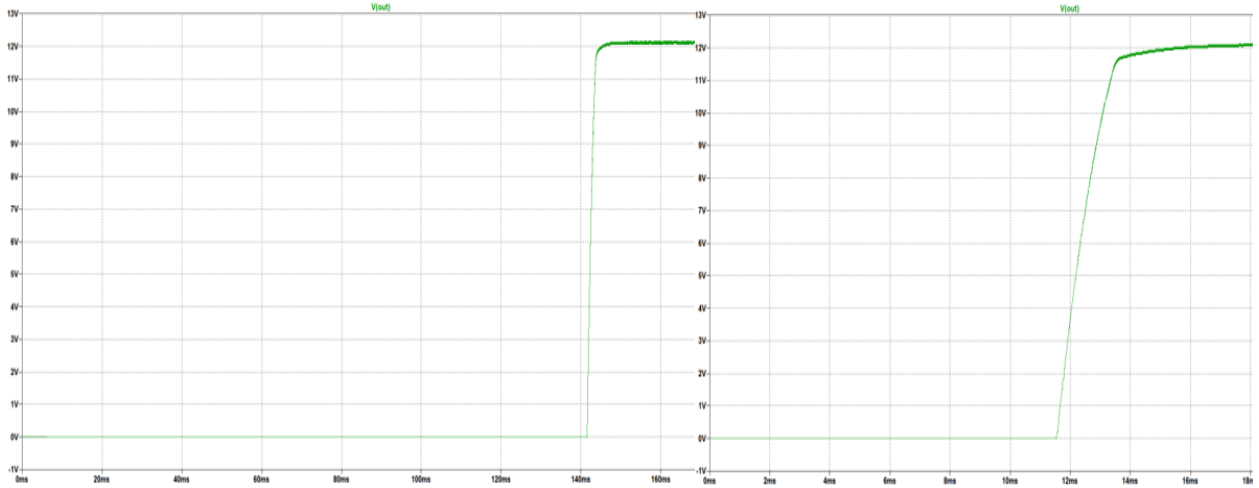


Figure 14 Output Voltage Waveform for 220V (left) and 400V (right) Input Voltage

The following Figure 15 shows the output voltage ripple both 220V and 400V input values.

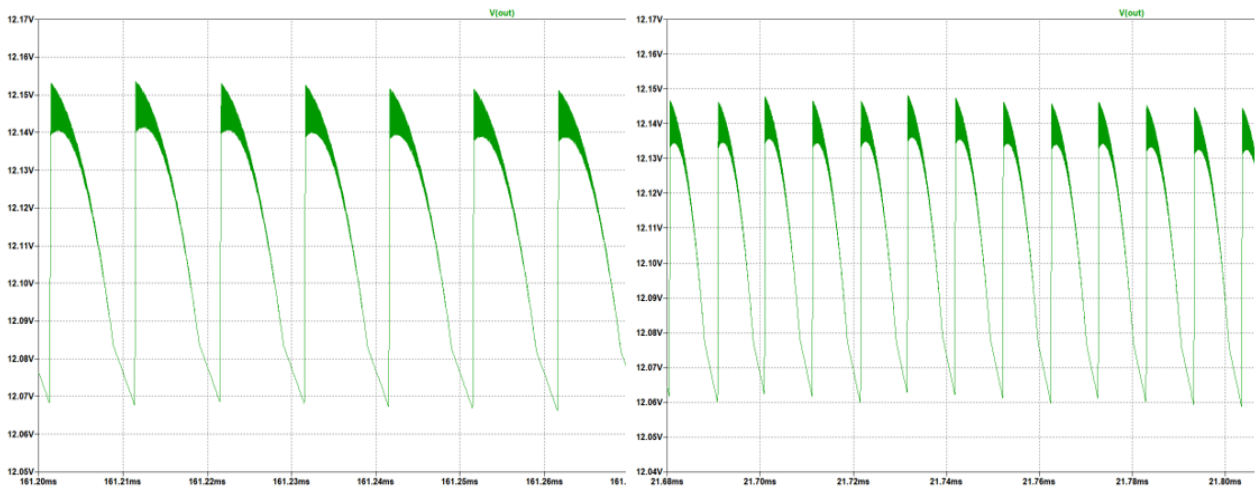


Figure 15 Output Voltage Waveform for 220V (left) and 400V (right) Input Voltage

The following Figures 16 and 17 show the performance of the design in the case of load regulation.

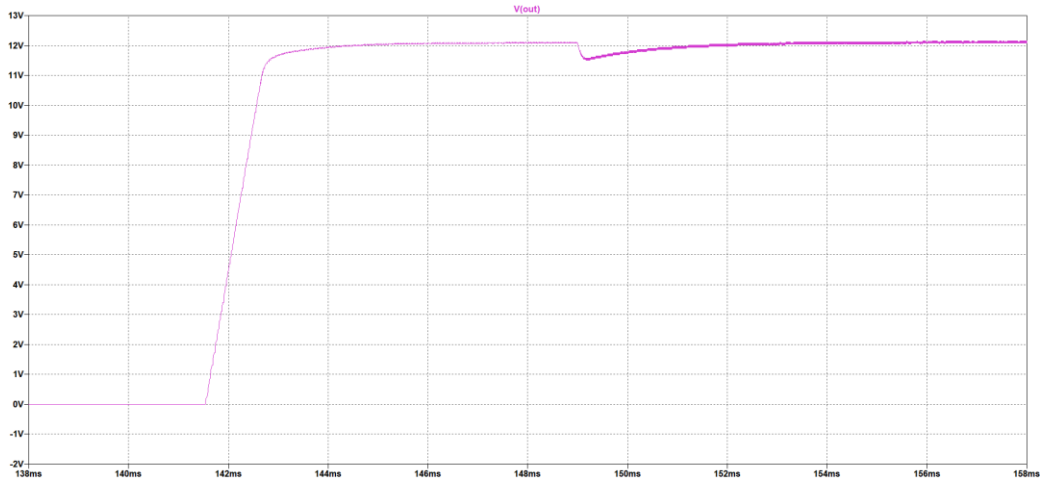


Figure 16 Load Regulation Performance of the Design

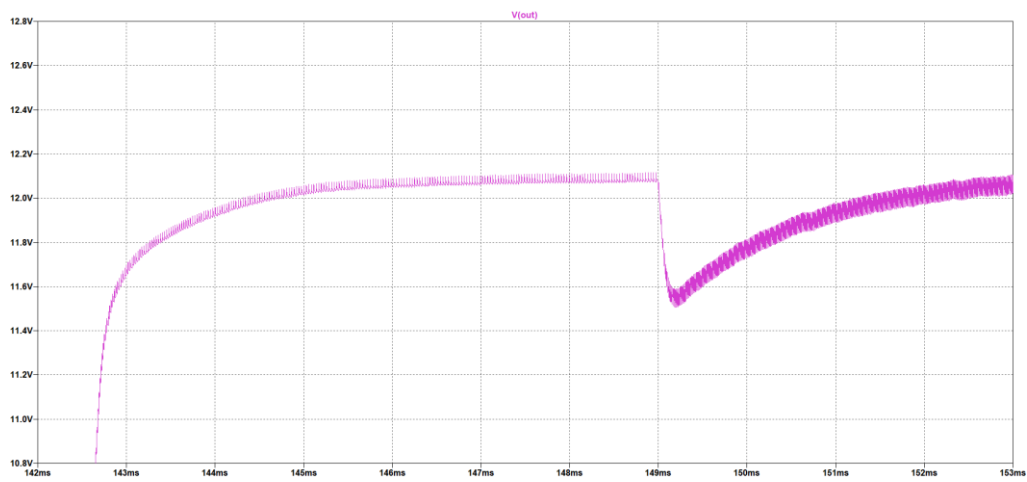


Figure 17 Output Voltage Drop against Load Regulation

It can be realized from the above figures, the voltage for this analysis is around 0.35V and this value is 3% of the output voltage. Hence, the project criterion is satisfied.

The current passing through the output capacitor which can be seen in the following Figure 18 is also important for the capacitor selection.

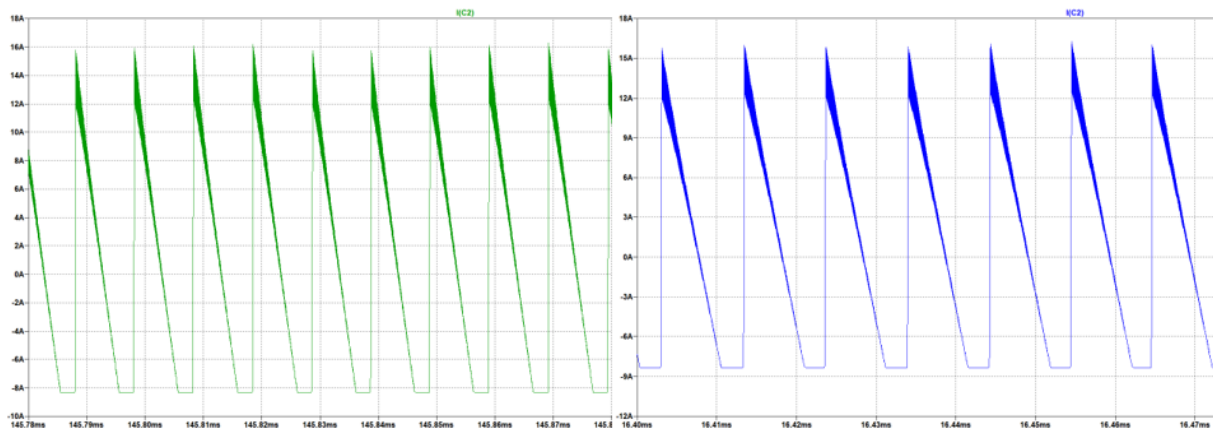


Figure 18 Output Capacitor Current Waveform for 200V (left) and 400V (right) Input Voltage

As can be seen in the above figures, the current ripple on this capacitor is almost 23A. Therefore, the selected capacitor for the output side should filter this ripple. Furthermore, to obey the 4% voltage ripple criterion the ESR value of the selected capacitor must be very small.

The following Figures 19 and 20 show waveforms of one of the output diode currents and the voltage on the diodes, respectively.

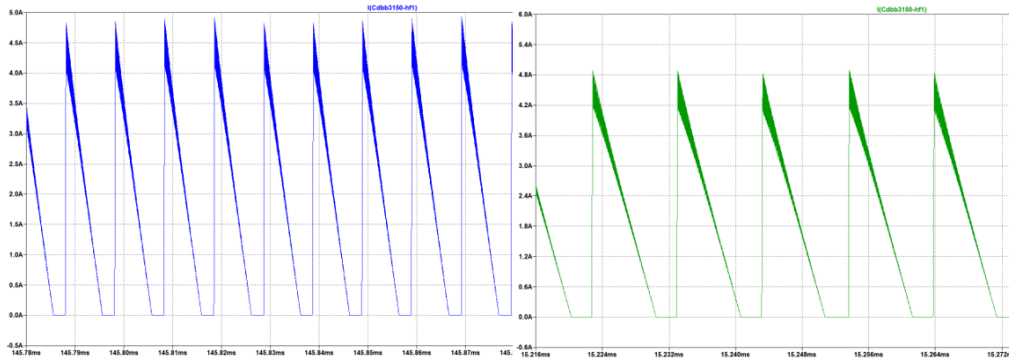


Figure 19 Output Diode Current Waveform for 200V (left) and 400V (right) Input Voltage

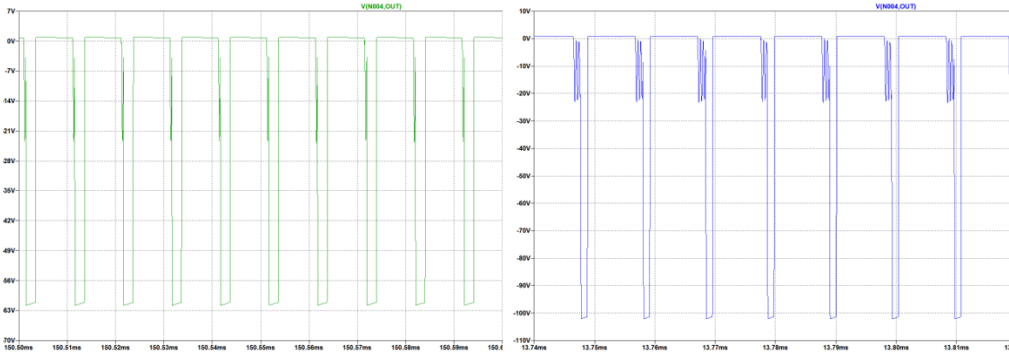


Figure 20 Output Diode Voltage Waveform for 220V (left) and 400V (right) Input Voltage

As can be seen in the above figures, one of the diode currents is almost the same for different input voltages and around 4.8A, and the total current on all the diodes is around 22A; however, the reverse voltages on these output diodes are not the same. When the input voltage is 400V, the diode can withstand almost 110V. These values are important for suitable output diode selection.

The following Figures 21 and 22 show the MOSFET gate voltage and current waveforms, respectively.

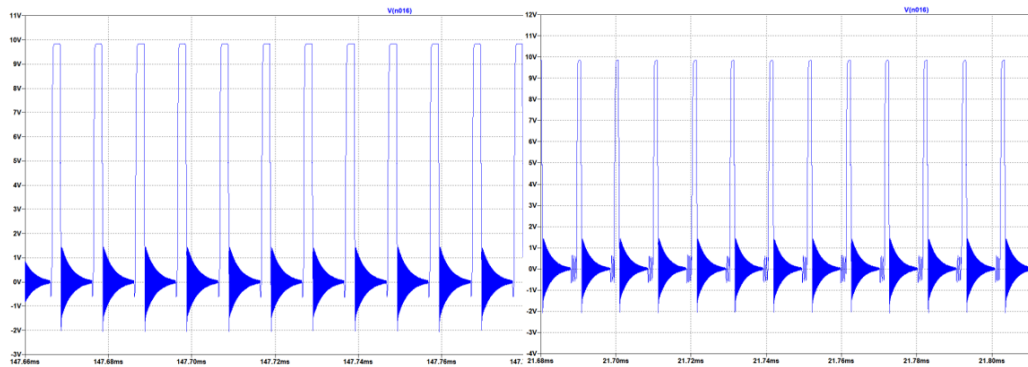


Figure 21 MOSFET Gate Voltage Waveform for 220V (left) and 400V (right) Input Voltage

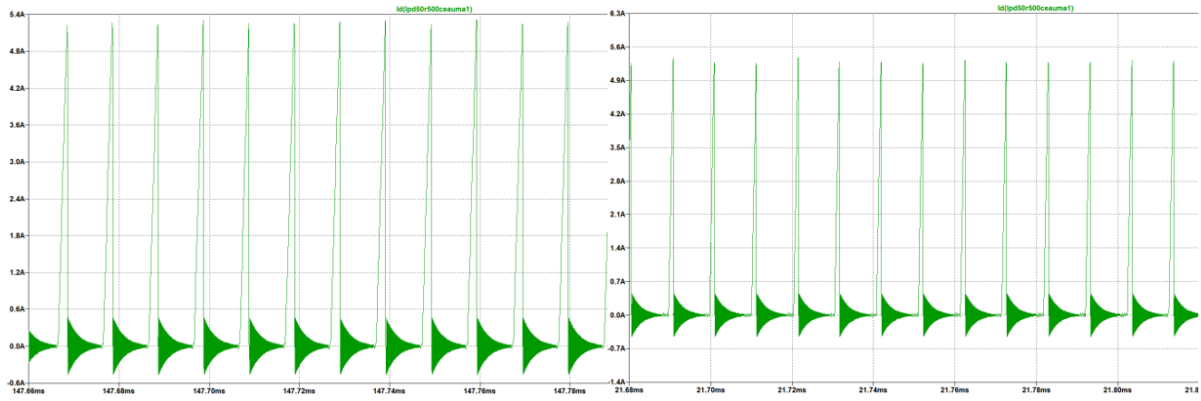


Figure 22 MOSFET Current Waveform for 200V (left) and 400V (right) Input Voltage

As can be seen in the above figures, the gate voltage of the MOSFET is almost the same for both cases and around 10V. Moreover, the current waveforms are also similar, and it is around 5.1A.

The following Figures 23 and 24 shows the voltage waveforms on the MOSFET with and without snubber circuit, respectively.

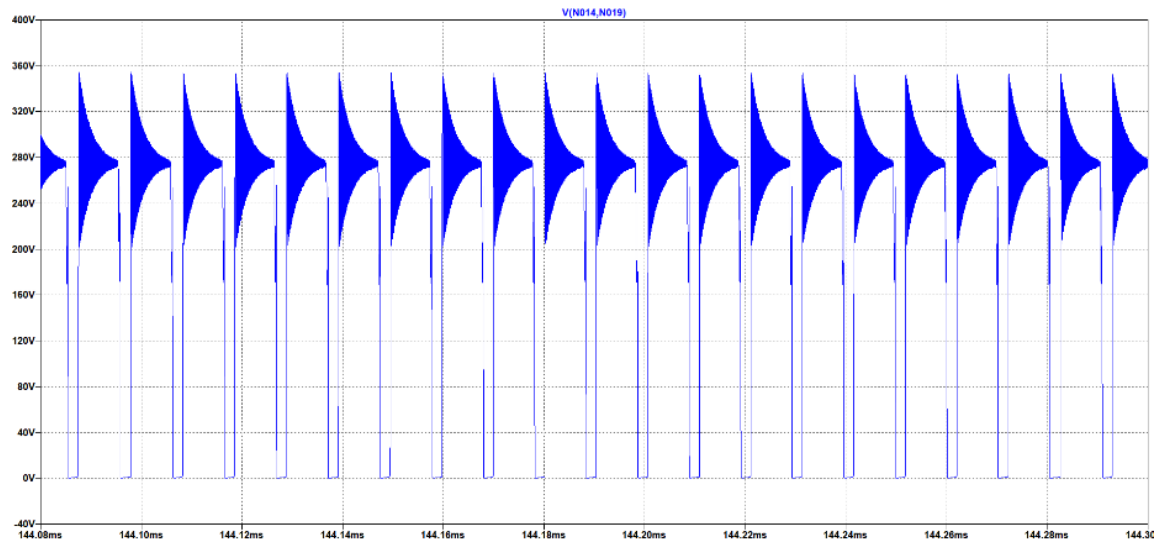


Figure 23 Voltage Waveform on the MOSFET with Snubber Circuit

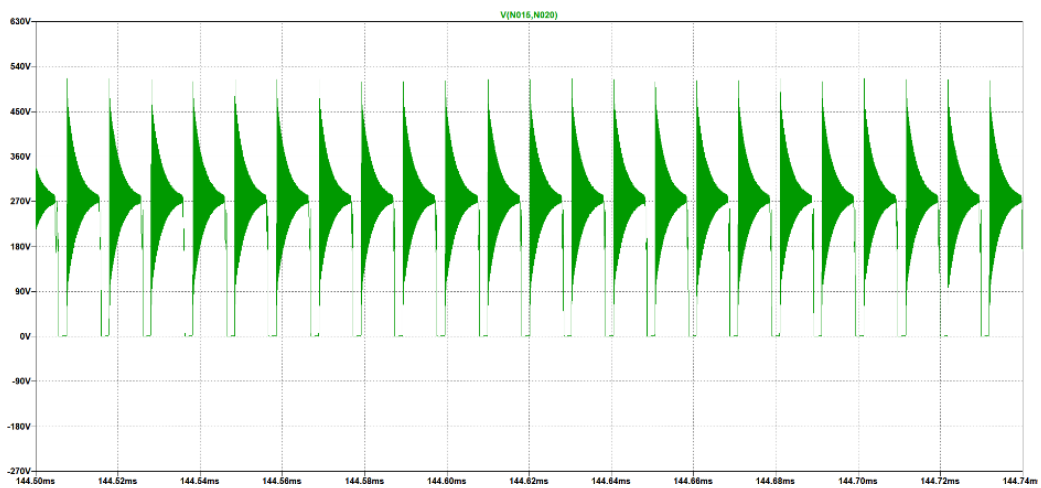


Figure 24 Voltage Waveform on the MOSFET without Snubber Circuit

As can be seen in the above figures, usage of snubber circuit decreases the voltage on the MOSFET up to 200V which allows us to select a lower rating MOSFET. On the other hand, the snubber circuit decreases the leakage inductance effect. Therefore, this snubber circuit usage is crucial.

In the following Figure 25, reverse voltage waveforms of the snubber diode can be seen.

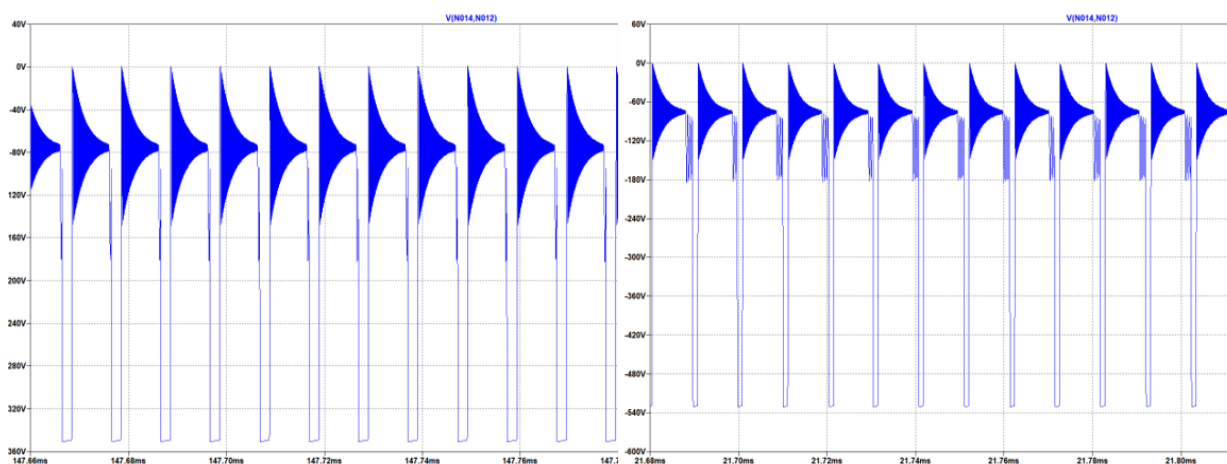


Figure 25 Snubber Diode Reverse Voltage Waveform for 200V (left) and 400V (right) Input Voltage

As can be seen in the above figure, the snubber diode reverse voltage is relatively high. That's why the selected diode can withstand 600V reverse voltage.

The following Figure 26 shows the power loss on the snubber resistance in Watt is shown for both 220V and 400V input voltage values.

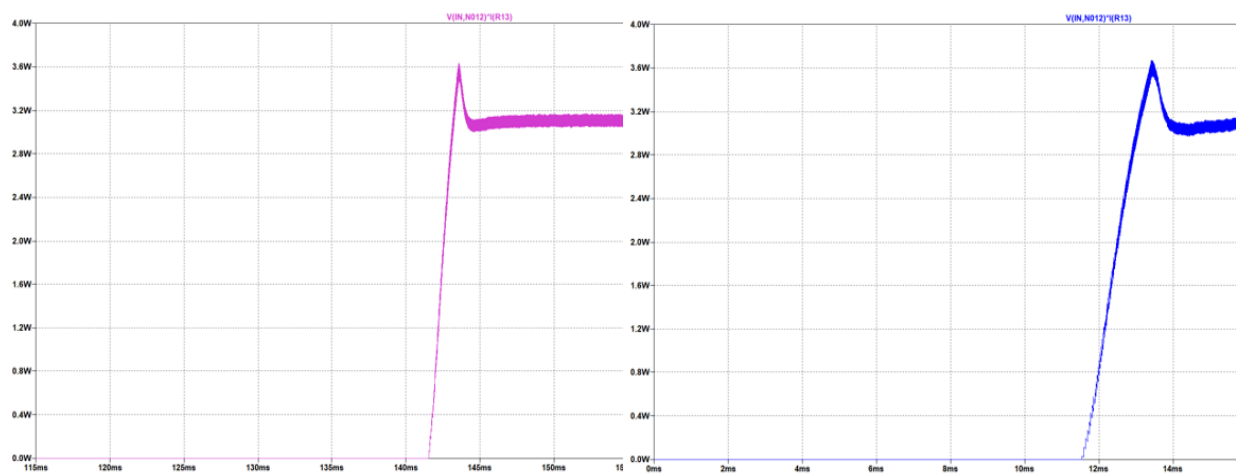


Figure 26 Power Losses on the Snubber Resistance for 220V (left) and 400V (right) Input Voltage

As can be realized from the above figure, there are some losses in the circuit. More detailed loss calculations can be seen in the following section of this report which is called “Loss Calculations”.

8. Loss Calculations

We know that $V_{in_{min}}$: 220 V, $V_{in_{max}}$: 400 V, V_{out} : 12 V, P_{out} 100 W from the project description. Also, the switching frequency is around 100kHz in both input voltage cases. This is known from both detailed simulations and controller features. Moreover, the transformer will produce magnetic and copper losses, therefore the transformer efficiency ratio will be taken as 0.9 in calculations. Output diode STPS30170DJF-TR has around 1 V forward voltage in secondary current ratings. Primary and secondary side power calculations are made as follows.

$I_{out_{avg}} = \frac{P_{out}}{V_{out}}, \quad I_{out_{avg}} = 8.333 \text{ A}$	(37)
$P_{diode} = V_F * I_{out_{avg}} = 8.333 \text{ W}$	(38)
$P_{secondary} = P_{out} + P_{diode} = 108.33 \text{ W}$	(39)
$P_{primary} = \eta_{transformer} = 120.367 \text{ W}$	(40)

Primary side switch power loss should be calculated to reach input power. Primary and secondary peak currents should be calculated to calculate switch power loss, therefore input power will be assumed as 125 W and analytical calculations will be compared with simulation results. Also, the transformer turns ratio is decided as 4.33 in magnetic design.

$V_{out} + V_{diode} = V_{in} \left(\frac{D}{1-D} \right) \left(\frac{N_2}{N_1} \right)$	(41)
$V_{in} = 220 \text{ V}, D = 0.21; V_{in} = 400 \text{ V}, D = 0.12$	(42)

Primary and secondary currents have a triangular shape.

$V_{in} = 220 \text{ V}, D_{max} = 0.21, \quad I_{in_{avg}} = \frac{P_{in}}{V_{in}} = 0.568 \text{ A}$	(43)
$I_{in_{peak}} = 2 * \frac{I_{in_{avg}}}{D_{max}} = 5.4 \text{ A}$	(44)
$V_{in} = 400 \text{ V}, D_{min} = 0.12, \quad I_{in_{avg}} = \frac{P_{in}}{V_{in}} = 0.3125 \text{ A}$	(45)
$I_{in_{peak}} = 2 * \frac{I_{in_{avg}}}{D_{min}} = 5.2 \text{ A}$	(46)

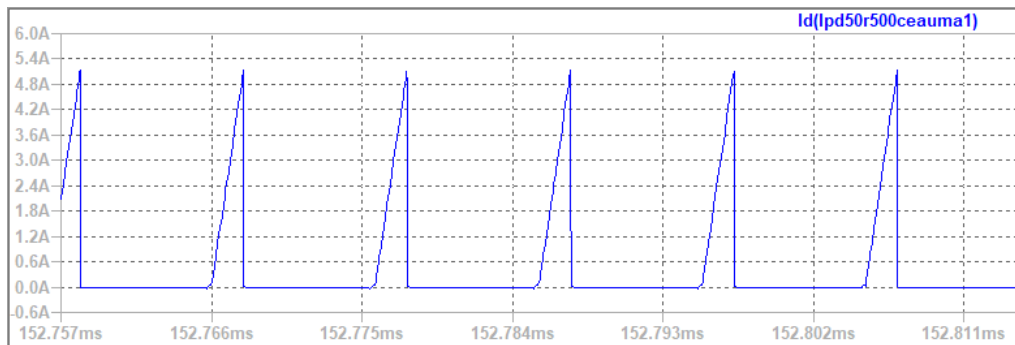


Figure 27 MOSFET Current Waveform ($V_{in}=220 \text{ V}$)

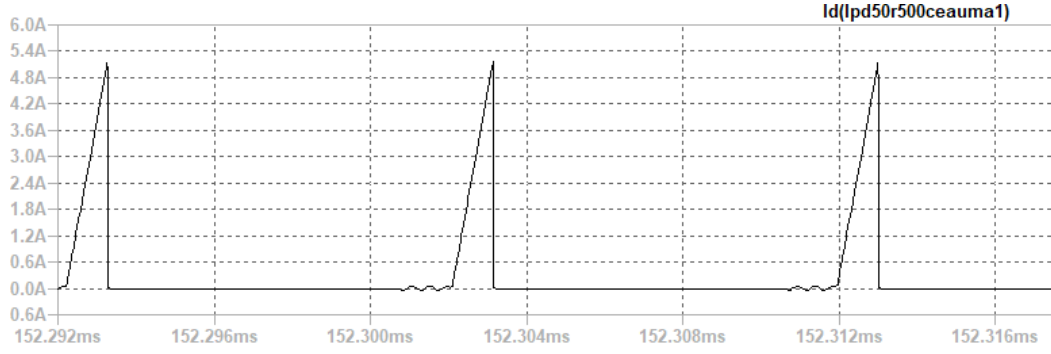


Figure 28 MOSFET Current Waveform ($V_{in} = 400\text{ V}$)

Input current rms value is used in the power loss calculation of MOSFET. It is calculated in LTspice as in Figure 29.

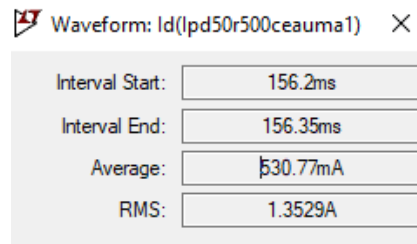


Figure 29 Maximum value of MOSFET current

Since the converter works in discontinuous conduction mode, we need to dwell time to calculate secondary side peak current. Dwell time is estimated from simulations as $0.05 \cdot D \cdot T_s$.

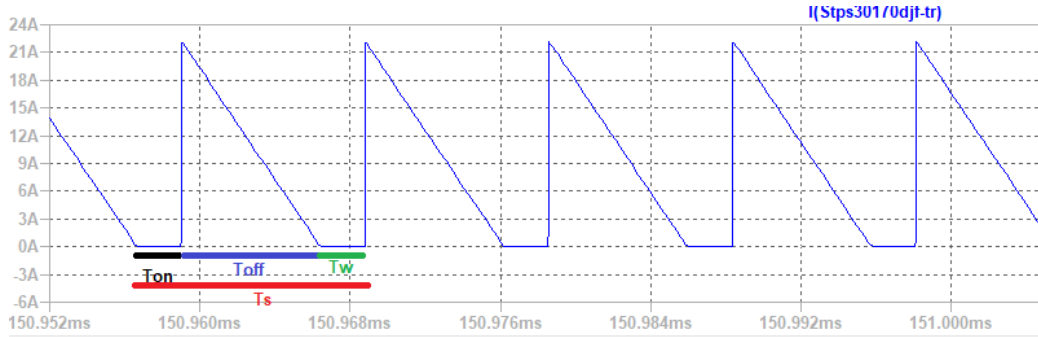


Figure 30 Secondary Side Diode Current

$$I_{sec_{peak(max)}} = 2 * \frac{I_{out_{avg}}}{(1 - D_{dwell} - D_{max})} = 22.52\text{ A} \quad (47)$$

Secondary side diode current value will be used in diode power loss, and it is calculated in LTspice.

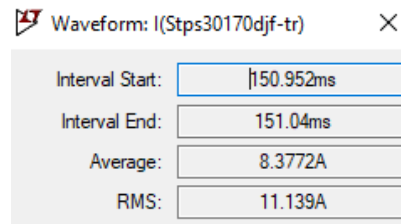


Figure 31 Maximum value of diode current

Voltage drop on MOSFET is calculated as follows.

$V_{sw} = Vin + \frac{N1}{N2} * Vout$	(48)
---------------------------------------	------

Table 4 Power Calculation Table

Loss mechanism	Component	Model
Conduction	MOSFET	$P_{on,M} = I_{in}^2 R_{on,M}$
Switching	MOSFET	$P_{sw,M} = \frac{1}{2} V_{sw} I_{in} (t_{rise} + t_{fall}) f_{sw}$
Switching – Output capacitance	MOSFET	$P_{coss} = \frac{1}{2} V_{sw}^2 (C_{DS} + C_{GD}) f_{sw}$ $P_{coss} = E_{coss} f_{sw}$
Switching – Gate charge	MOSFET	$P_G = Q_g V_{gs} f_{sw}$
Switching	MOSFET Diode	$P_{bodydiode} = \frac{1}{2} V_{sw} I_{RR} t_{RR} f_{sw}$
Conduction	Diode	$P_{on,D} = V_f I_{out}$
Conduction – Copper loss	Transformer	$P_{copper} = I_{in,rms}^2 R_{pri} + I_{out,rms}^2 R_{sec} + I_{third}^2 R_{third}$
Magnetic Loss	Transformer	$P_{core} = a * (f^x) * (B_{op}^y) * V_{core}$
Conduction	Shunt resistor	$P_{shunt} = I_{in,rms}^2 R_{shunt}$
RCD Snubber	Resistor-Diode	$P_{on,D} = V_f I_{RCD}, P_{shunt} = I_{RCD,rms}^2 R_{RCD}$

The maximum R_{DS} value is 0.5 Ω in MOSFET Datasheet, therefore the worst case is calculated in MOSFET conduction loss. $t_{rise} + t_{fall}$ time is 19ns in the worst case, therefore the worst case is calculated in MOSFET switching losses. Typical $E_{coss} = 2.2 \mu J$, it is taken in the calculation of output capacitance power loss. The maximum Gate threshold voltage of the MOSFET is 3.5V. The total gate charge of the MOSFET is 18.7nC. Also, the body diode of the MOSFET is taken into consideration while making calculations and its related values are taken from the datasheet. In the design, instead of using a single diode and collecting all losses in a single diode, 5 diodes are connected in parallel, and it reduces the loss per diode also the use of heat sinks is avoided. Output diode has 0.75 V on voltage while it is conducting 1.66A per diode. Also, the output diode has not to reverse recovery loss since it a Schottky diode. Magnetic loss parameters are taken from the Magnetics website. While calculating copper losses of the transformer, the third winding is also taken into consideration, however, there is very little current on the third winding, therefore it did not affect the losses much. In the wiring design, the expected loss value was 1.5 W when the normal wiring was done first, and the copper loss decreased to 0.1 W thanks to the Litz wire. The worst-case for the RCD snubber circuit occurs when the input voltage is low, that is, more current is flowing on the primary side, because the leakage inductor will store more energy. In this circuit, the resistor consumes the most power. In the worst case, the RCD circuit consumes 3 Watts of power, the resistor's characteristics can meet this situation.

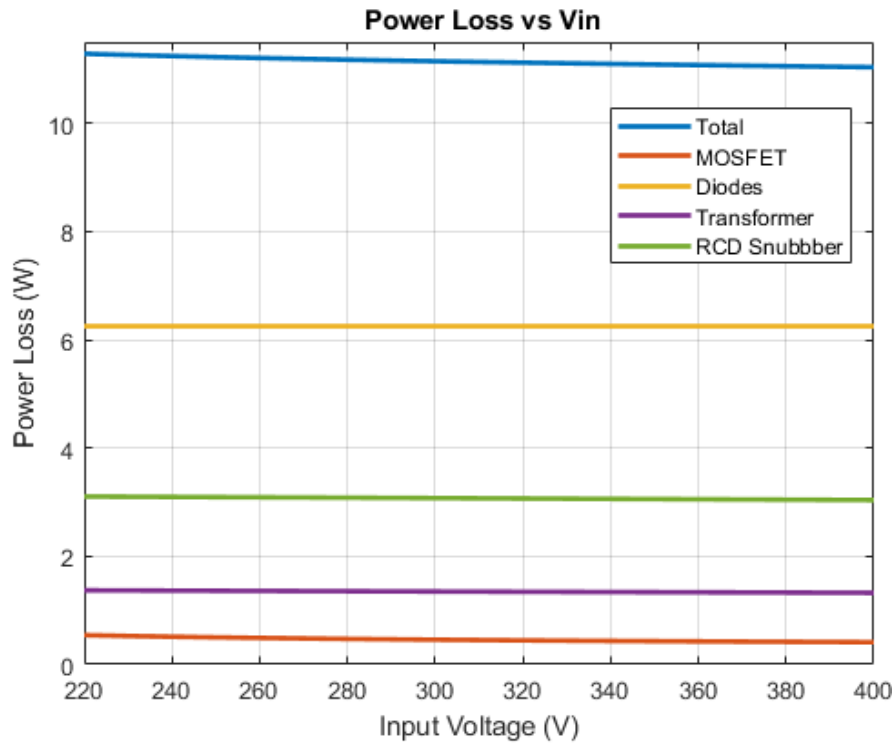


Figure 32 Power Loss vs Input Voltage

According to the power calculation table, the losses with respect to the input voltage values are shown in Figure 32. Maximum power loss is 11.28 W; thus the expected minimum efficiency of the system is %89.86. As the input voltage drops, the input current will increase since the transferred power is constant, so the losses on the primary side will increase. Thus, efficiency increases as the input voltage increases.

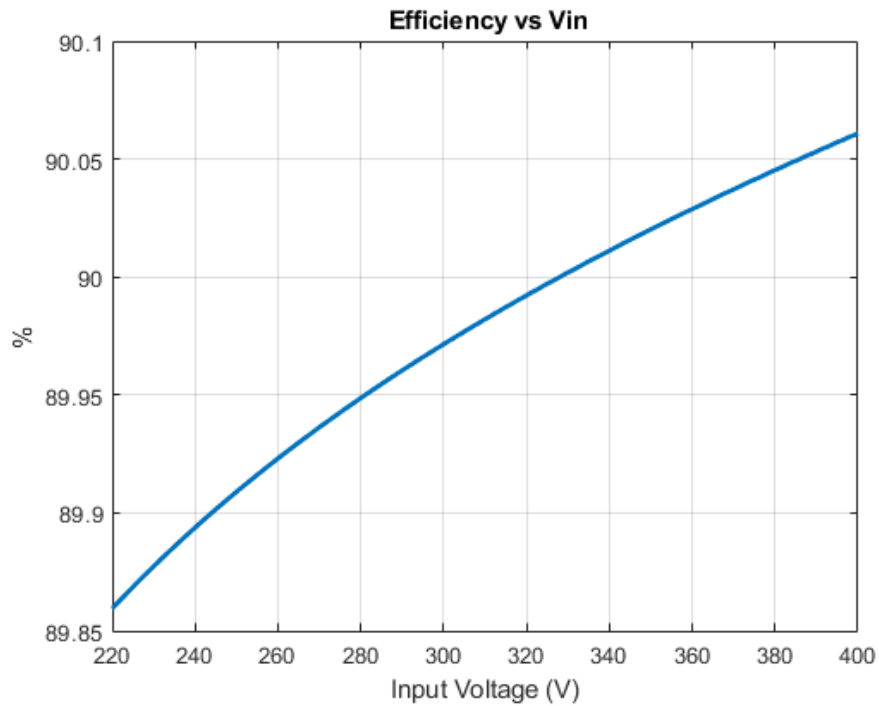


Figure 33 Efficiency vs Input Voltage

9. Thermal Calculations

The following Figure 34 shows the schematic of junction temperature without a heatsink. Also, junction–case thermal resistance should be added to the system.

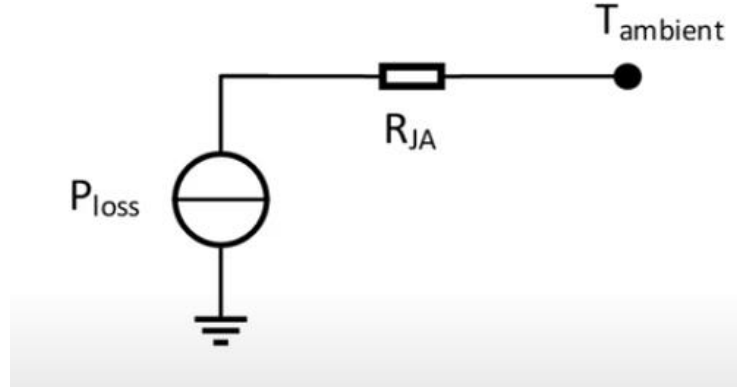


Figure 34 Schematic of Junction Temperature without Heatsink

The following Figure 35 shows the schematic of junction temperature with heatsink.

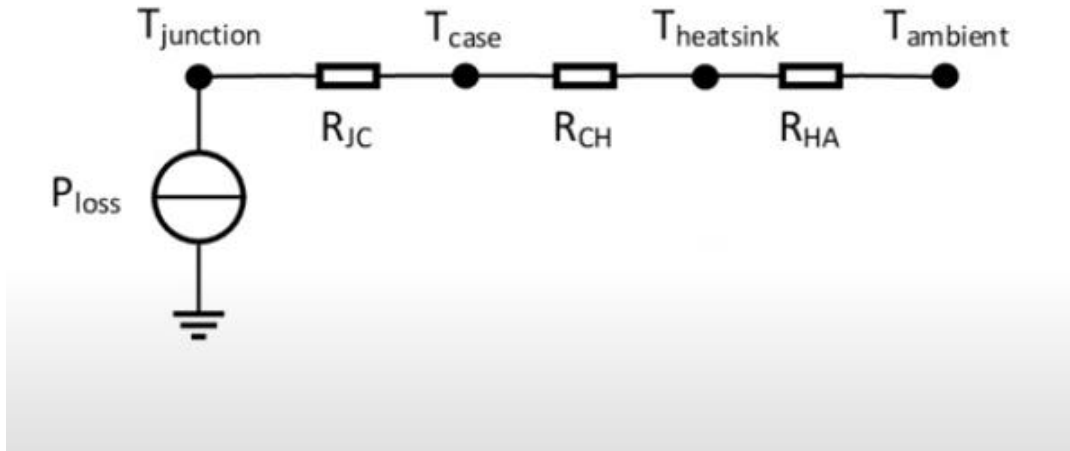


Figure 35 Schematic of Junction Temperature with Heatsink

Junction temperature without heatsink can be calculated with Equation 49 and junction temperature with heatsink can be calculated with Equation 50. Moreover, if a lower junction temperature is needed, a heatsink can be used. Required thermal resistance for the heatsink can be calculated as in Equation 51.

$T_{junc} = T_{ambient} + P_{loss} * R_{JA}$	(49)
$T_{junc} = T_{ambient} + P_{loss} * (R_{JC} + R_{CH} + R_{HA})$	(50)
$R_{HA} = \frac{T_{junc} - T_{ambient}}{P_{loss}} - R_{JC} - R_{CH}$	(51)

9.1. MOSFET

Ambient temperature is assumed as 25°C and junction temperature is calculated as follows. When R_{DS} is 0.50Ω, the calculated maximum power loss is 0.54 W.

$R_{thJA,TYP} - R_{thJA,MAX}: 35^{\circ}C/W - 62^{\circ}C/W$			
R_{DS}	Assumed T_J	Max. Power Loss	Calculated max T_J
0.50Ω	25°C	0.54 W	58°C
0.60Ω	58°C	0.57 W	60.3°C
0.61Ω	60.3°C	0.58W	61°C
0.61Ω	61°C	0.58W	61°C

The most important feature of the MOSFET we use is that it causes low losses. R_{DS} value is both very low and its value does not change much with increasing temperature, also low losses have been obtained due to low current values in the primary side. Thanks to all this, no heatsink is required for the MOSFET since MOSFET can operate up to 150°C.

9.2. Diode

Instead of using a single diode for the output diode, 5 diodes are connected in parallel. Also, since the Schottky diode is connected, there is no switching loss. The maximum loss on the diodes is 1.64 W per diode. The junction to ambient resistance of the diode used is 55 °C/W.

$T_{junc} = 25^{\circ}C + 1.64 * 55 = 115.2^{\circ}C,$	$T_{ambient} = 25^{\circ}C$	(52)
$T_{junc} = 40^{\circ}C + 1.64 * 55 = 130.2^{\circ}C,$	$T_{ambient} = 40^{\circ}C$	(53)

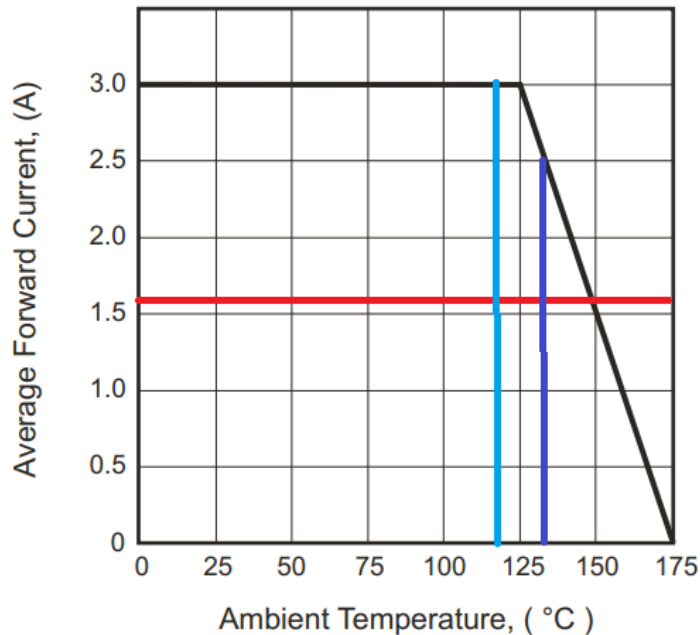


Figure 36 Typical Forward Current Derating Curve

The current value per diode is 1.66A and as can be seen in figure X, the diode can provide sufficient current at the calculated junction temperature values.

Moreover, there is no need to calculate the thermal behavior of the snubber diode since snubber diodes just consume 15mW.

10. Hardware Design

10.1. Schematic Design

In this project, we have designed a schematic for the Flyback Converter hardware, by considering detailed simulation with LT8316 and DC2718A Demo Board Schematic, which is a 16V-600V input, 12V-3A output Flyback Converter demo board with LT8316. As a consequence of having a capable controller and tertiary winding transformer, we do not need any digital isolator (i.e. optocoupler) between two isolation boundaries. So, we have concluded our schematic with the controller, transformer, connectors, and some discrete components (discussed in the component selection part) such as resistors, capacitors, diodes. We have not needed any extra ICs. Compared with the Simulation Report, some of the components have changed in schematic design and they are discussed in the Component Selection and Controller Part.

In the component selection part, we have discussed feedback resistors, UVLO resistors, and sense resistors for the controller. There are some additional recommended components, that we placed in our schematic design. We can have a short discussion about these components:

IntVcc Pin: This pin is to maintain the internal supply voltage that is taken from the Bias pin. To do that, the datasheet recommends a minimum 2.2uF capacitor, in the schematic we have placed a 4.7uF capacitor.

Bias Pin: This pin takes the internal supply voltage from tertiary windings, so the datasheet recommends a bypass capacitor to the ground. We have placed a 4.7uF ceramic capacitor, again.

Smoke Pin: This pin is used for stand-by operation. To avoid that we have connected it to the ground.

Vc Pin: This pin is the Loop Compensation pin, which determines the switching frequency from the feedback voltage. The datasheet recommends an R-C network to stabilize the regulation generally with a 20kohm resistor and 220nF capacitor. Normally decreasing R-value and increasing C value causes transient problems and increasing R-value and decreasing C value causes high-frequency problems. However, when we examine the demo board discussed above, the R-C network is constructed with a 15kohm resistor and 100nF capacitor. When comparing these values with the datasheet recommendation, we see that the demo board application gives better transient values, so a 15kohm resistor and 100nF capacitor have been used in the hardware design.

I_{REG}/SS Pin: This pin helps to regulate the output current. From this pin, 10uA current flows, and with the connected resistor, the voltage drop on the pin adjusts the current regulation. When we look datasheet, a formula is provided for this pin's resistor, so when we calculate the needed resistor for 8.33A output current, we see that we need to connect a 50kohm resistor between this pin and ground.

TC Pin: This pin is used for Temperature Compensation, and from this pin to the feedback pin, a temperature compensation resistor is connected. Normally, there is a temperature coefficient that is found experimentally from the output diode voltage and temperature change, then the required resistance of this pin is calculated from this coefficient. However, in this

project we are not able to implement that test, so we will use the demo board's TC resistor which is 121kohm.

In addition to these recommended components by the datasheet, we have used some additional components, which are input ceramic capacitors to compensate high-frequency problems from input, and we have used a MOSFET gate resistor to limit the dI/dT ratio of gate current, and lastly, we have used a gate pull-down resistor to prevent any failure which may occur from the controller. Moreover, we have added a TVS diode to prevent overvoltage cases, discussed in the component selection part.

In Figure 37, we can see the input connector and the input bypass capacitors, in Figure 38, we can see the output connector, and finally, in Figure 39, we can see the schematic design of our Flyback Converter and controller.

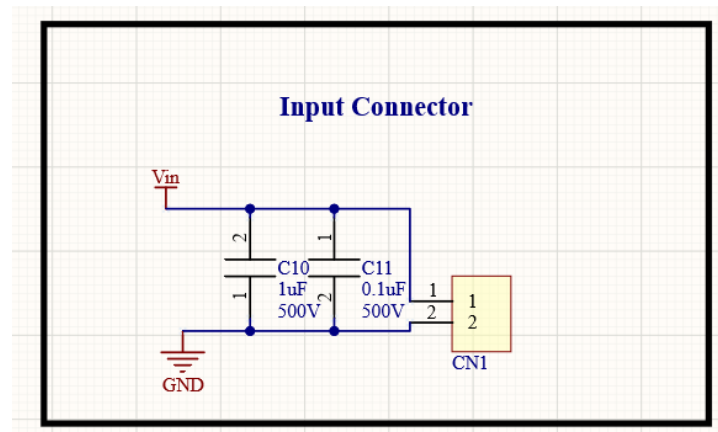


Figure 37 Input Connector and Input Bypass Capacitors

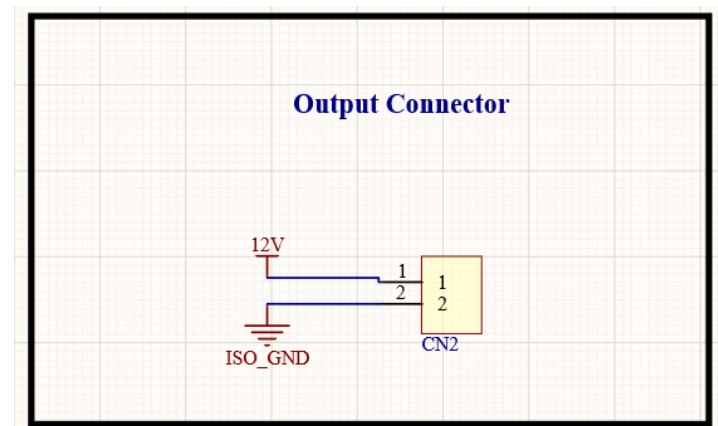


Figure 38 Output Connector

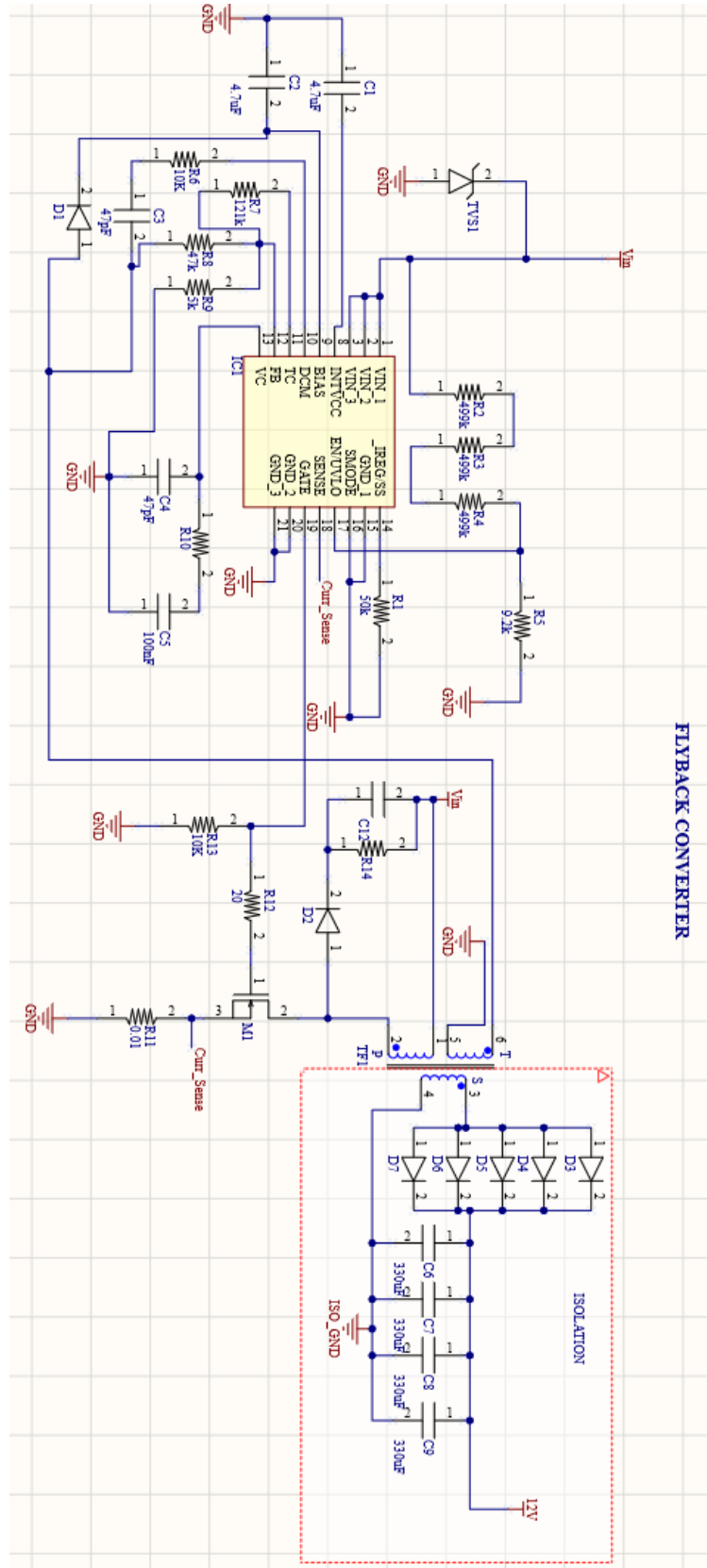


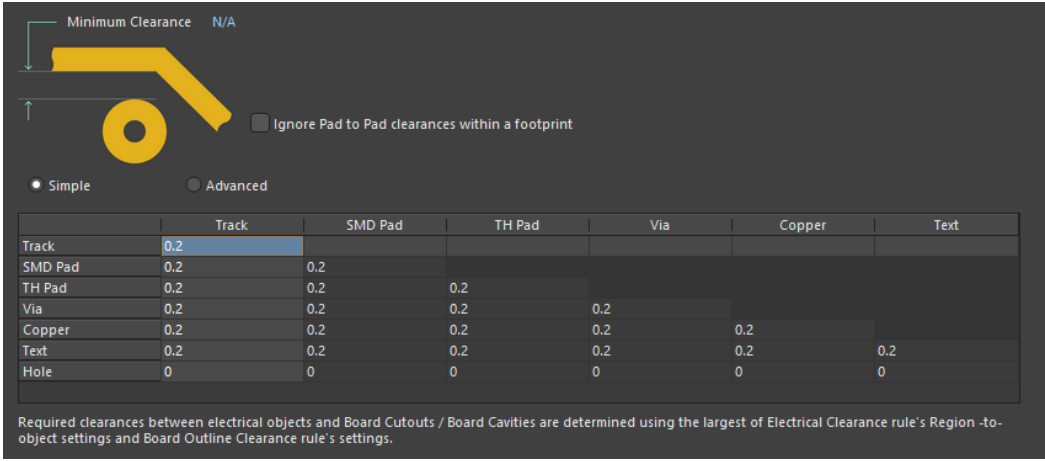
Figure 39 Flyback Converter and Controller

10.2. PCB Design

a. Rules and Validations

After concluding our Simulation Report and feedback session, we have made some changes on components, performed power, and thermal analysis, and started to design our PCB. While designing our PCB, our main idea was to have a compact, reliable, and cheap product. Among all these properties, safety was the leading property.

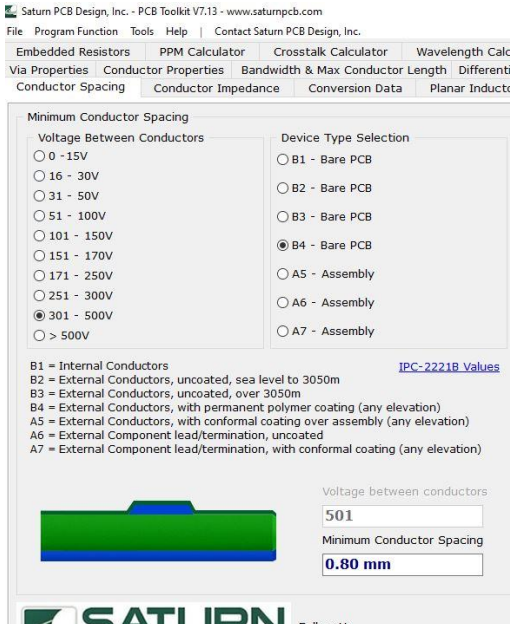
While designing this project, we have used Altium Designer 20, and our design is two-layered and both layers include components. Before starting to draw, we have determined to design rules which can be seen in Figure 40. Moreover, according to IPC2221A between 300V-500V, the clearance between two points should be 2.5mm for safe design. However, if the PCB has conformal coating this clearance can be decreased down to 0.8mm, so we have designed our PCB in this manner. This 0.8mm clearance is validated from Saturn PCB Toolkit and can be seen in Figure 41.



	Track	SMD Pad	TH Pad	Via	Copper	Text
Track	0.2					
SMD Pad	0.2	0.2				
TH Pad	0.2	0.2	0.2			
Via	0.2	0.2	0.2	0.2		
Copper	0.2	0.2	0.2	0.2	0.2	
Text	0.2	0.2	0.2	0.2	0.2	0.2
Hole	0	0	0	0	0	0

Required clearances between electrical objects and Board Cutouts / Board Cavities are determined using the largest of Electrical Clearance rule's Region -to-object settings and Board Outline Clearance rule's settings.

Figure 40 Design Rules from AD20



Minimum Conductor Spacing

Voltage Between Conductors

- ☐ 0 - 15V
- ☐ 16 - 30V
- ☐ 31 - 50V
- ☐ 51 - 100V
- ☐ 101 - 150V
- ☐ 151 - 170V
- ☐ 171 - 250V
- ☒ 251 - 300V
- ☐ 301 - 500V
- ☐ > 500V

Device Type Selection

- ☐ B1 - Bare PCB
- ☐ B2 - Bare PCB
- ☐ B3 - Bare PCB
- ☒ B4 - Bare PCB
- ☐ A5 - Assembly
- ☐ A6 - Assembly
- ☐ A7 - Assembly

B1 = Internal Conductors
 B2 = External Conductors, uncoated, sea level to 3050m
 B3 = External Conductors, uncoated, over 3050m
 B4 = External Conductors, with permanent polymer coating (any elevation)
 A5 = External Conductors, with conformal coating over assembly (any elevation)
 A6 = External Component lead/termination, uncoated
 A7 = External Component lead/termination, with conformal coating (any elevation)

IPC-2221B Values

Voltage between conductors: 501

Minimum Conductor Spacing: 0.80 mm

SATI IDN

Figure 41 Conformal Coating Clearance Validation

From Detailed Simulations, we know that the input current goes up to 5A. In this manner, we need to validate the line width and via properties for the worst case, which is 5A. On the input side, the minimum width for the current-carrying path is 1.3mm, and from Figure 42 we can see that this line accepts up to 6.5A current. This means that we are in a safe zone for line width.

The screenshot shows the Saturn PCB Design, Inc. - PCB Toolkit V7.13 interface. The 'Conductor Characteristics' tab is active. The 'Solve For' section has 'Conductor Width' selected. The 'Plane Present?' section has 'Yes' selected. The 'Parallel Conductors?' section has 'No' selected. The 'Options' section has 'Base Copper Weight' set to 18um, 'Plating Thickness' set to 18um, and 'Conductor Layer' set to 'External Layer'. The 'Units' section has 'Metric' selected. The 'Substrate Options' section has 'Material Selection' set to 'FR-4 STD'. The 'Er' is 4.6 and 'Tg (°C)' is 130. The 'Temp Rise (°C)' is 40. The 'Temp in (°F)' is 72.0. The 'Ambient Temp (°C)' is 50. The 'Temp in (°F)' is 122.0. The 'Information' section shows 'Total Copper Thickness' as 36 um, 'Via Thermal Resistance' as N/A, 'Via Count' as 10, and 'Conductor Temperature' as N/A. The 'Print' and 'Solve!' buttons are visible.

Parameter	Value
Conductor Width	1,3 mm
Conductor Length	10 mm
PCB Thickness	1,6 mm
Frequency	0,2 MHz
Distance to Plane	0,254 mm
IPC-2152 with modifiers mode	Etch Factor: 1:1
Skin Depth	147.59435 um
Power Dissipation	0.25464 Watts
Conductor DC Resistance	0.00597 Ohms
Skin Depth Percentage	100%
Power Dissipation in dBm	24.0592 dBm
Conductor Cross Section	0.046 Sq.mm
Voltage Drop	0.0390 Volts
Conductor Current	6.5302 Amps

Figure 42 Line Width Validation

The screenshot shows the Saturn PCB Design, Inc. - PCB Toolkit V7.13 interface. The 'Via Characteristics' tab is active. The 'Via Hole Diameter' is 0,3 mm, 'Via Height' is 1,6 mm, and 'Via Plating Thickness' is 0,035 mm. The 'Options' section has 'Base Copper Weight' set to 18um, 'Plating Thickness' set to 18um, and 'Property Selection' set to 'Via Properties'. The 'Units' section has 'Metric' selected. The 'Substrate Options' section has 'Material Selection' set to 'FR-4 STD'. The 'Er' is 4.6 and 'Tg (°C)' is 130. The 'Temp Rise (°C)' is 40. The 'Temp in (°F)' is 72.0. The 'Ambient Temp (°C)' is 50. The 'Temp in (°F)' is 122.0. The 'Information' section shows 'Power Dissipation (dBm)' as 12.2801 dBm, 'Via Thermal Resistance' as 110.2 °C/W, 'Aspect Ratio' as 5.33:1, 'Via Count' as 10, and 'Via Temperature' as 11.0 °C/W per via. The 'Print' and 'Solve!' buttons are visible.

Parameter	Value
Via Hole Diameter	0,3 mm
Via Height	1,6 mm
Via Plating Thickness	0,035 mm
Via DC Resistance	0.00118 Ohms
Power Dissipation	0.01690 Watts
Via Inductance	1.2993 nH
Conductor Cross Section	0.0368 Sq.mm
Via Current	3.7846 Amps

Figure 43 Via Validation

Lastly, when we look at design rule validation of our design, which can be seen in Figure 44, we do not see any errors, which means all of the components, lines, and vias are placed with respect to rules, and we have a safe design.

Date: 24.06.2021
Time: 20:31:25
Elapsed Time: 00:00:02
Filename: C:\Users\ASUS\Desktop\5-2\EE464\Term Project\Project\EE464_Project\EE464_PCB.PcbDoc

Warnings: 0
Rule Violations: 0

Figure 44 Design Rule Check

b. 2D Design

To have a high-power density design, we have placed the components into both layers. When we look from the top view, the left-hand side is the high voltage side and the right-hand side is the isolated (low voltage) side. The overall view of the PCB design can be seen in Figure 45.

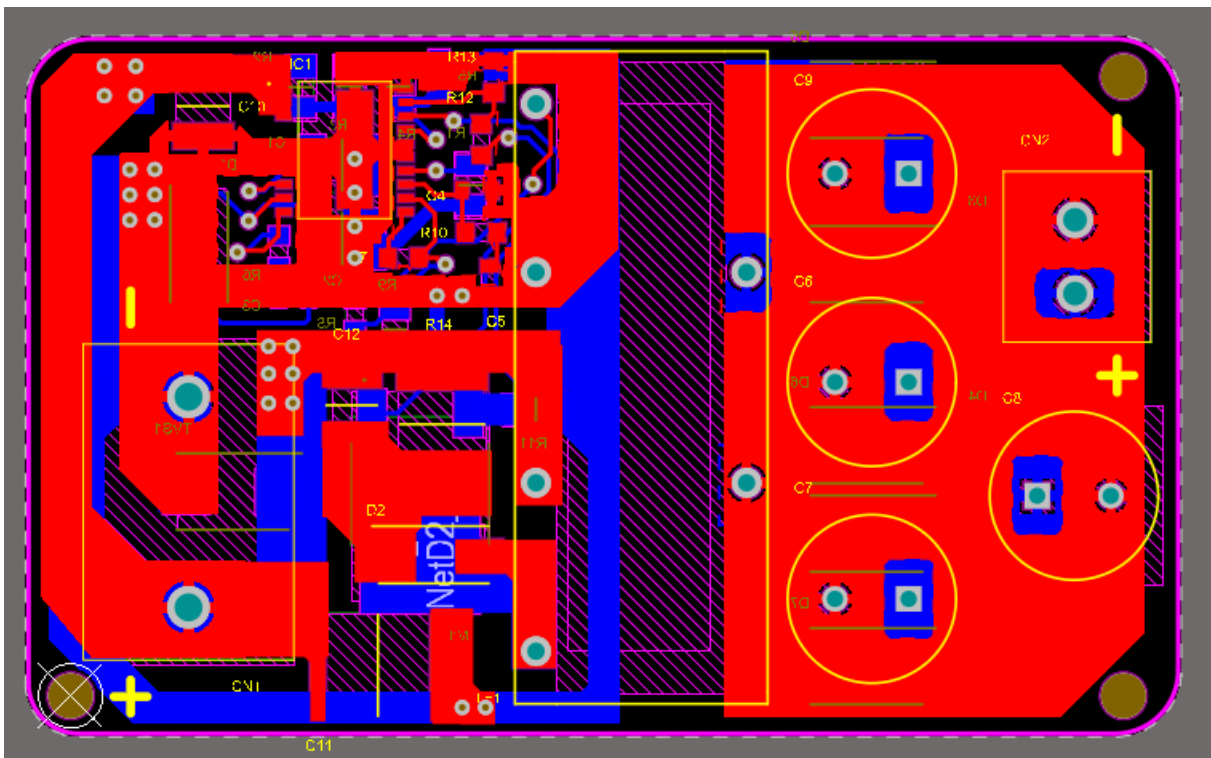


Figure 45 Overall View of PCB

To understand our design, we need to investigate component placements and plane placements. Firstly, we will investigate the isolation side, and we will refer high voltage side as the **input side**, and the low voltage output side as the **isolated side**, which can be seen in Figure 46, and then we will investigate component placements. In Figure 47 we can see the top layer and in Figure 48 we can see bottom layer component placements.

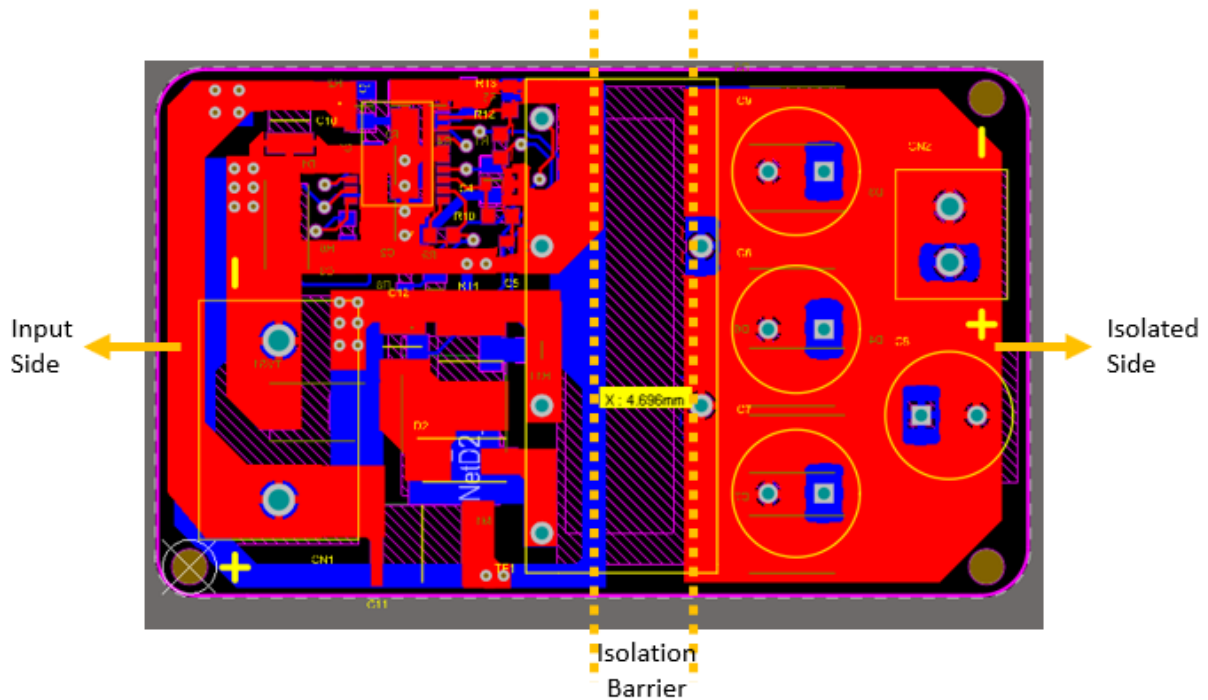


Figure 46 Top Layer Component Placement

As seen in Figure 46, between two isolated planes we have nearly 4.7mm. According to IPC-2221B, this spacing is suitable for 940V reference difference for uncoated PCBs and 1750V reference difference for coated PCBs, we have designed our board with conformal coating, so which means our design is safe. As seen above, we have no connections between the two sides, so no interactions between two isolated planes.

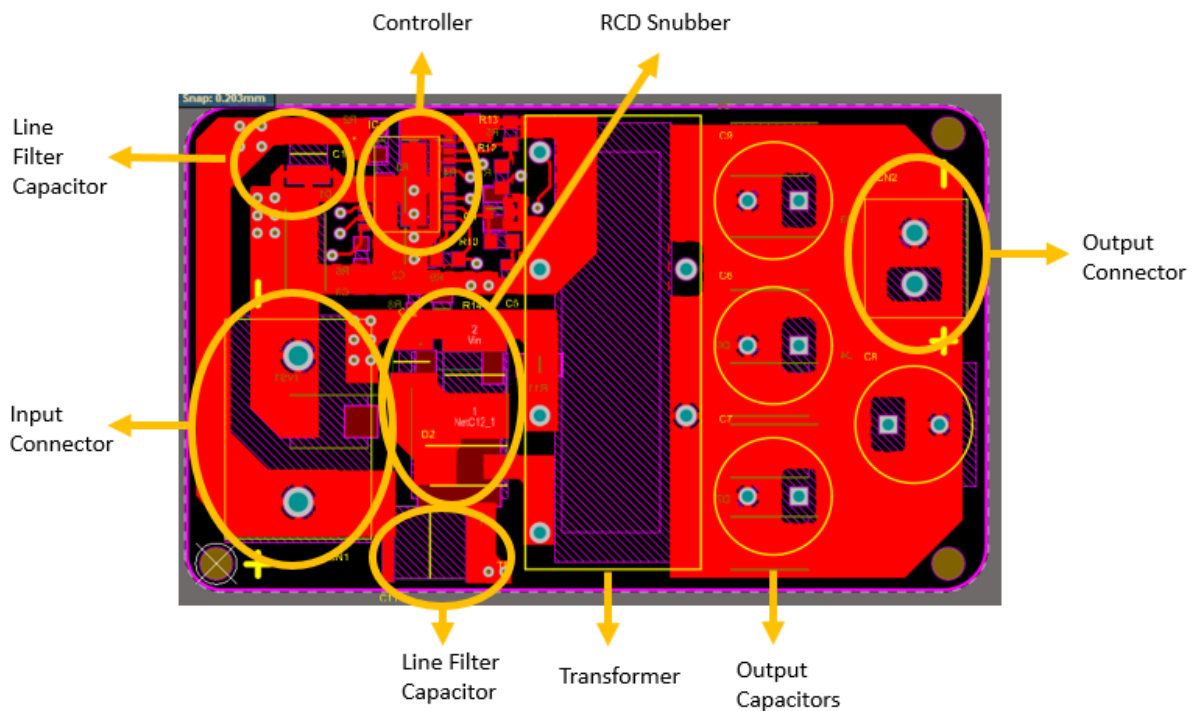


Figure 47 Top Layer Component Placement

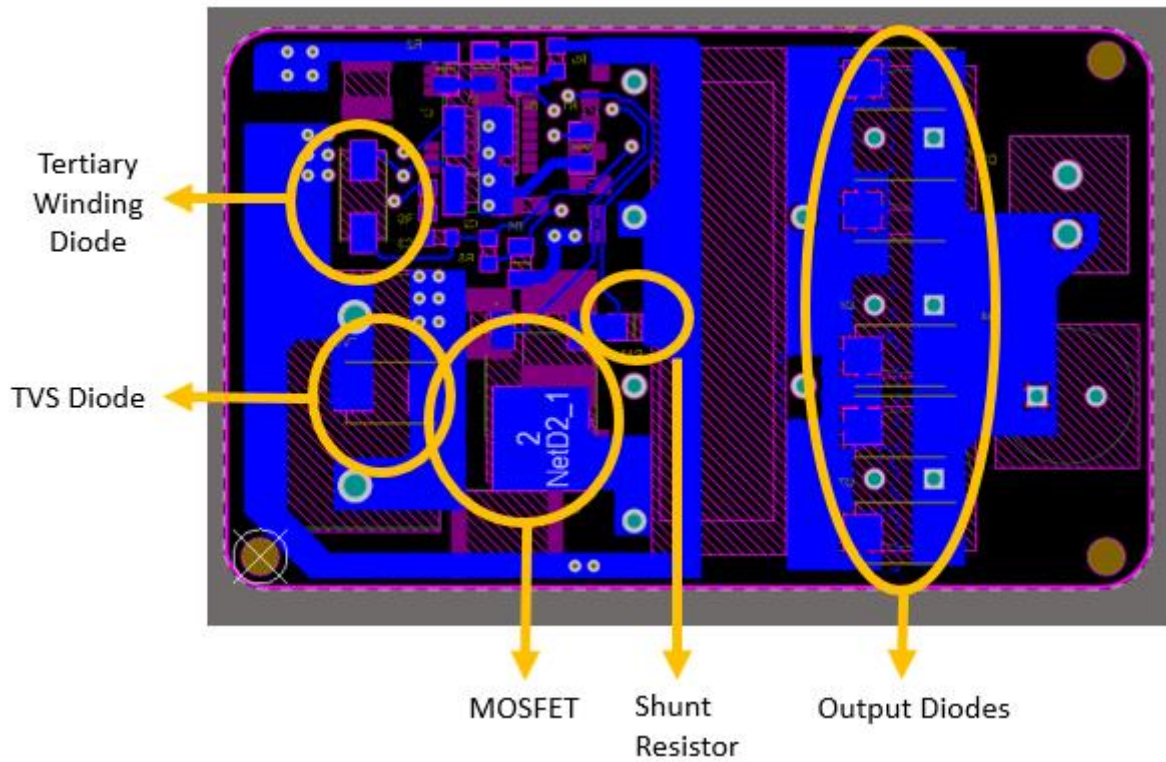


Figure 48 Bottom Layer Component Placement

After investigating critical component placements, we need to look at plane placements for top and bottom layers to understand the whole PCB. In Figure 49 and Figure 50, we can investigate plane placements for top and bottom layers, respectively.

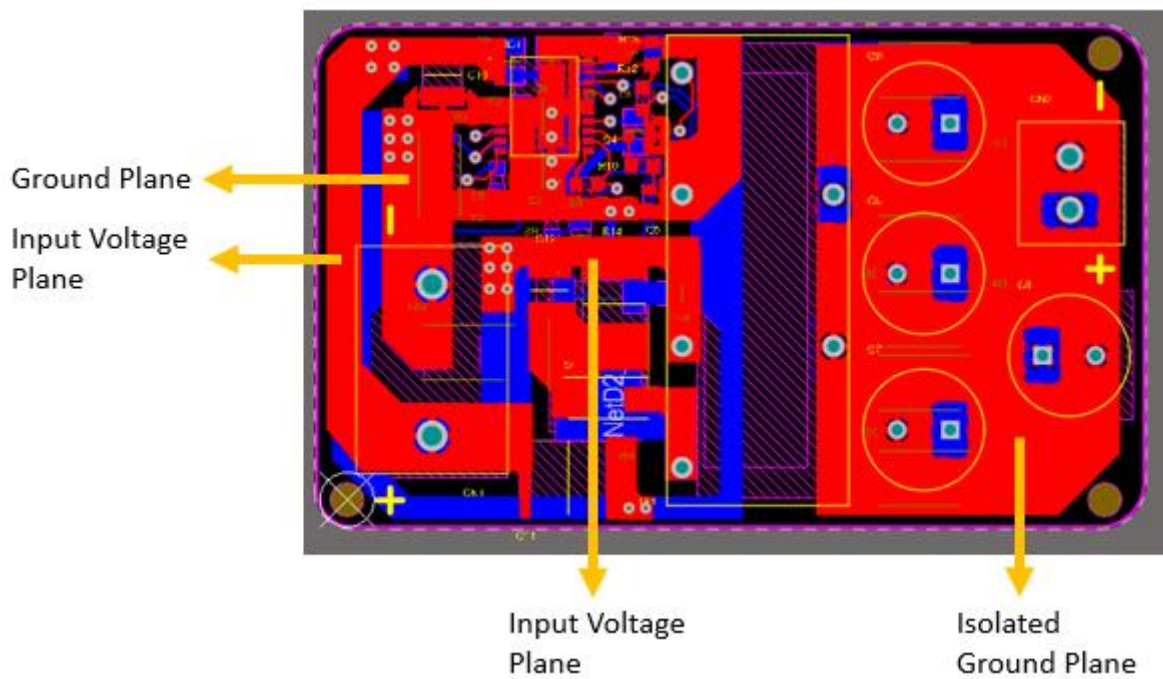


Figure 49 Top Layer Plane Placement

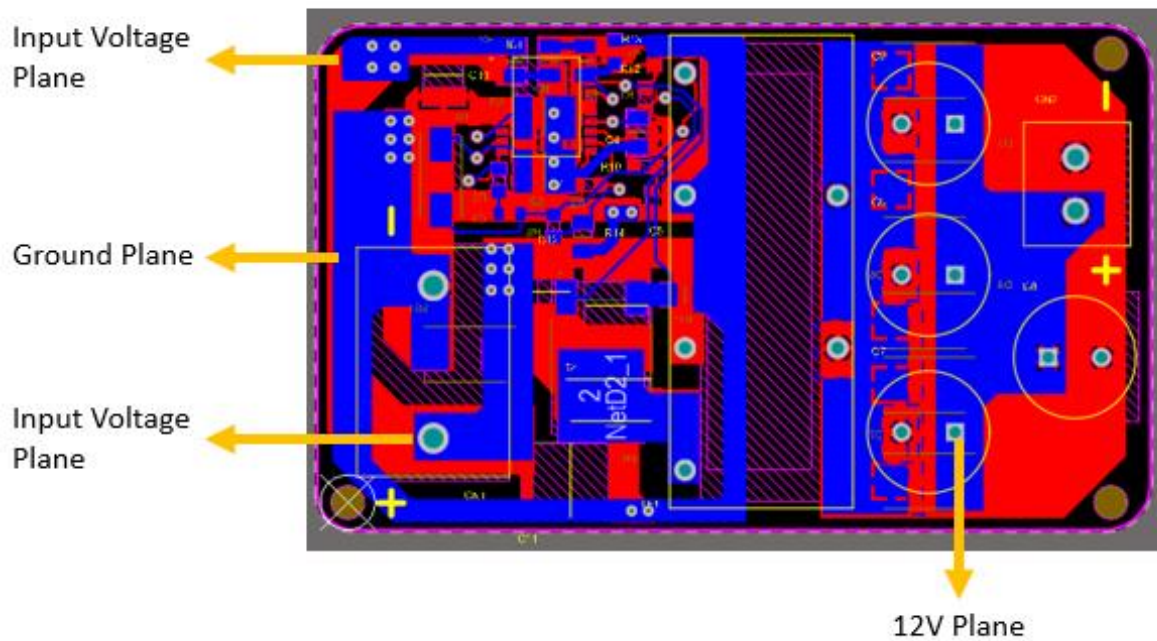


Figure 50 Bottom Layer Plane Placement

Lastly, when we look at the mechanical properties of the board, it has dimensions of **54.6mm x 33mm**, which is a quite small board compared with its properties. The board dimensions can be seen in Figure 51. Moreover, when we look at this figure, we will see the **fiducials** that are placed on board to ease manufacturing and **positive/negative terminal indicators** of connectors for safety.

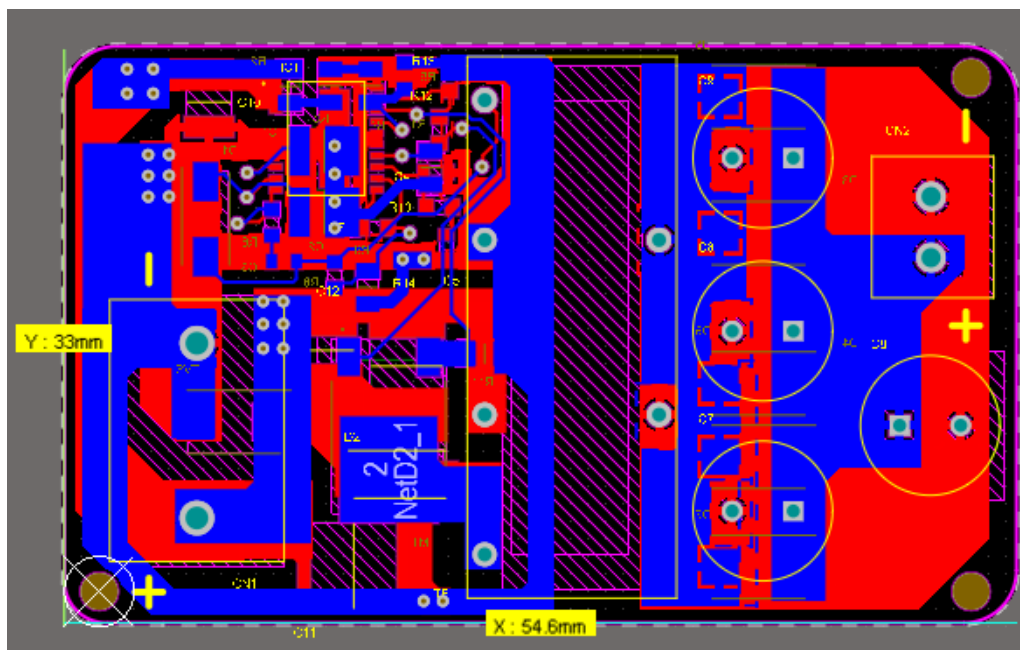


Figure 51 Board Dimensions and Mechanical Properties

c. 3D Design

In our design, we have placed all of the 3D bodies of components to have a realistic and reliable design. As we mentioned before, to have a compact design we placed the components on both top and bottom layers. The 3D design can be seen in Figures 52, 53, and 54.

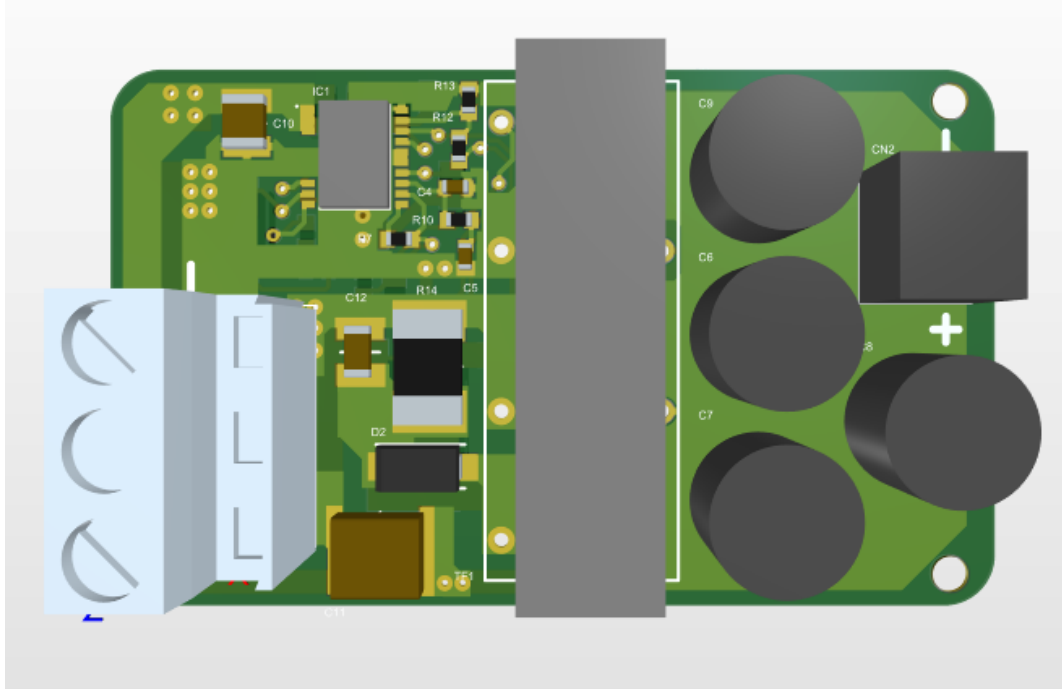


Figure 52 Top View of 3D PCB Design

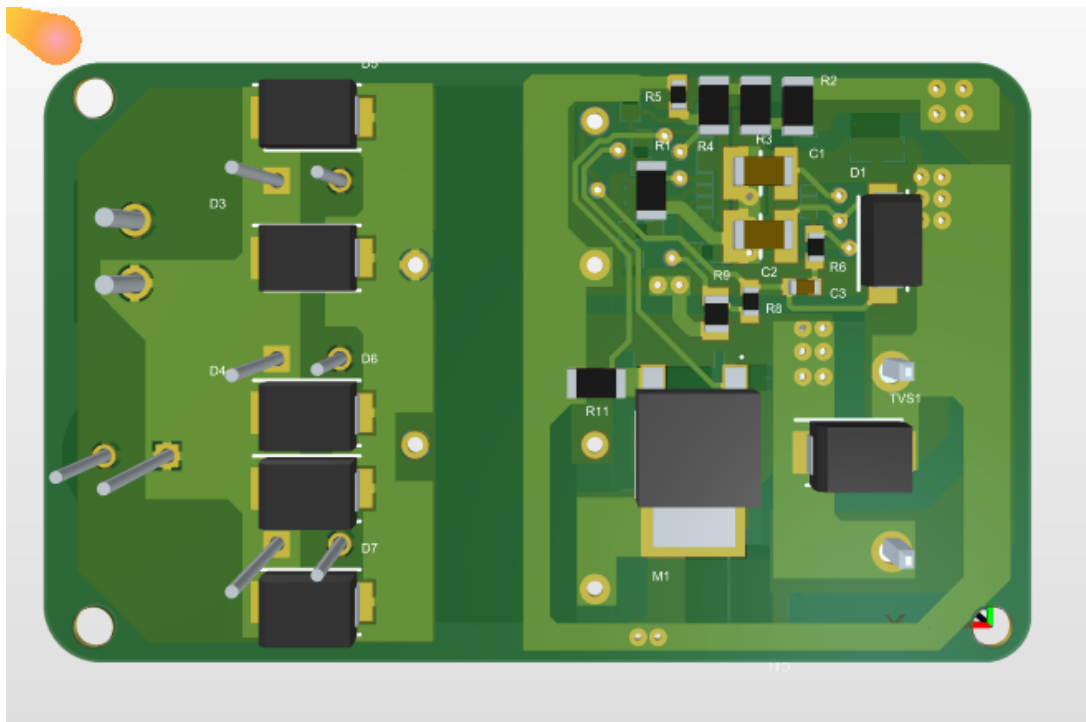


Figure 53 Bottom View of 3D PCB Design

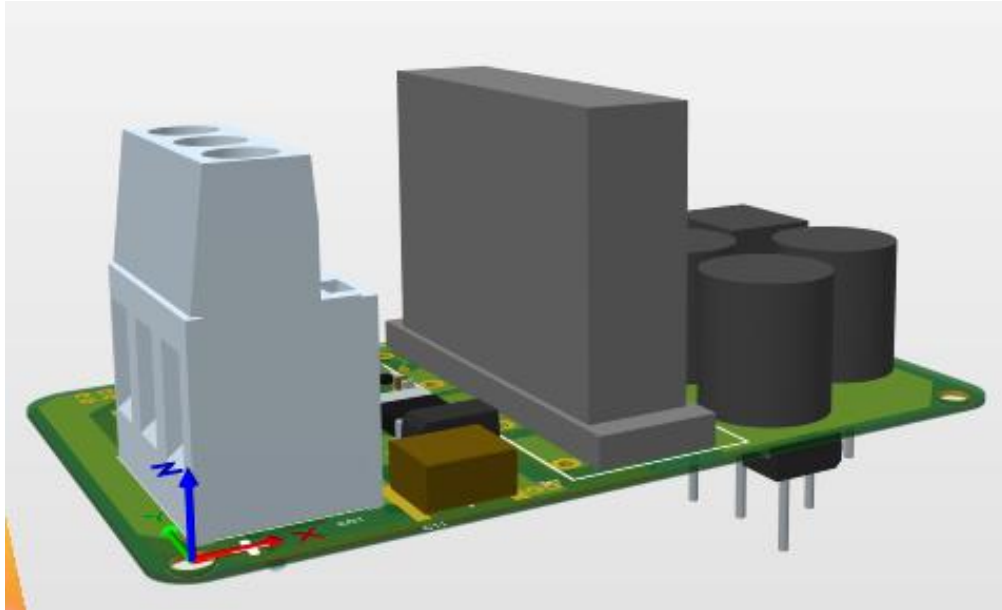


Figure 54 Side View of 3D PCB Design

In the 2D Design part, we have shown the component placement. However, to realize the PCB design better, component placements in 3D design can be seen in Figures 55 and 56 for top view and bottom view, respectively.

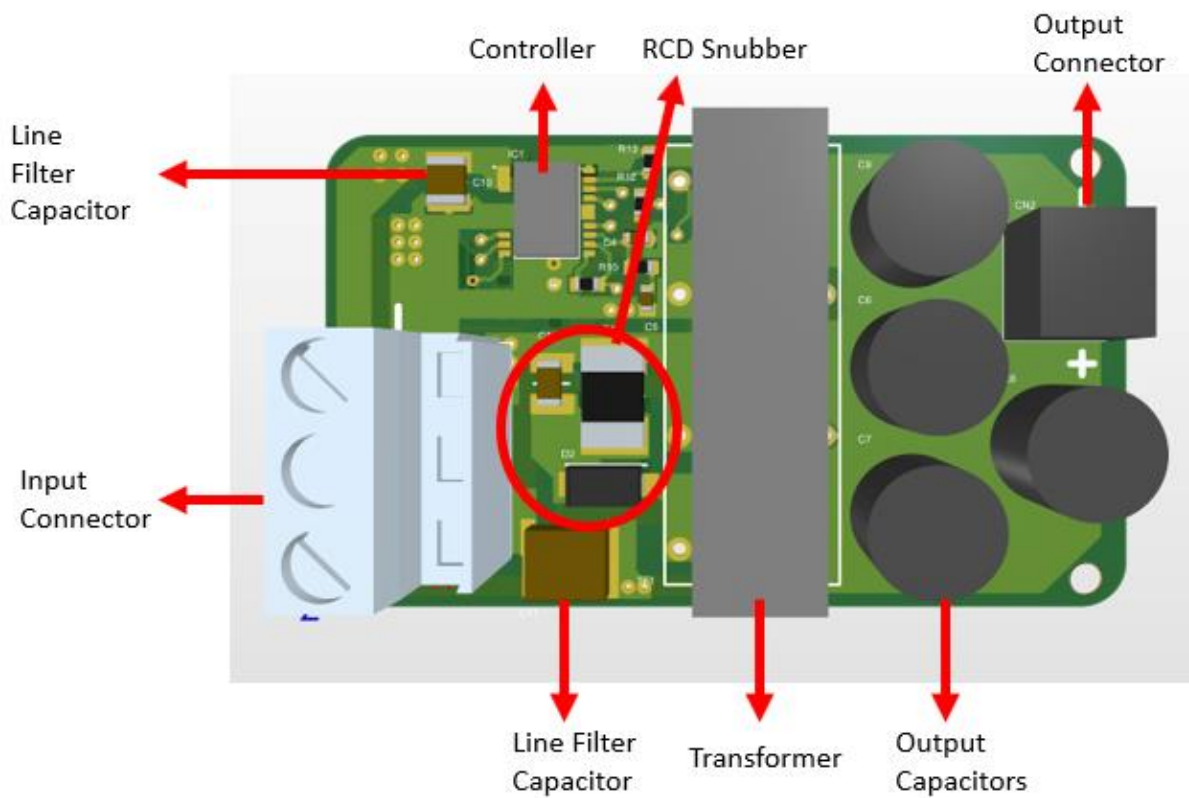


Figure 55 3D Design Top Layer Component Placement

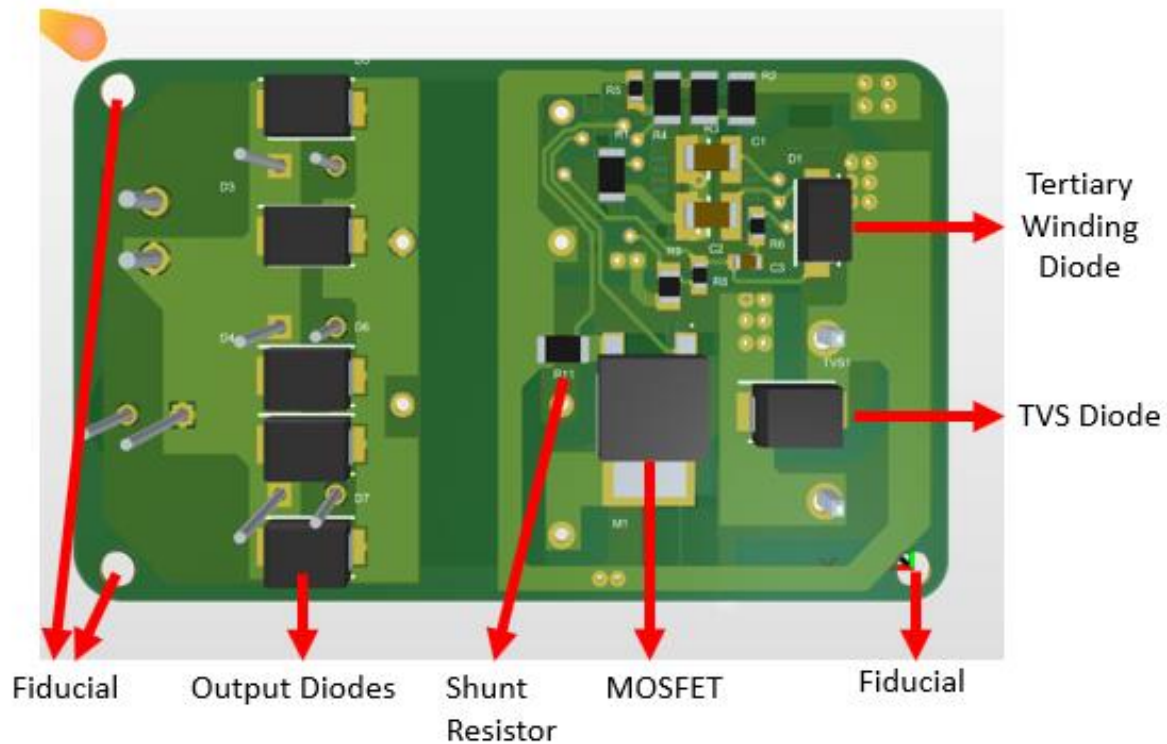


Figure 56 3D Design Bottom Layer Component Placement

In this project, we have designed the board for 18um base copper and 18um plating thickness, and we have made all of the clearance validation calculations in this manner. The total board thickness is 1.6mm and the used material is FR-4 because FR-4 material is commonly used. After all, it is more efficient compared with Aluminum and more resistant to water exposure. The transition temperature (T_g) is selected as 130-140 to have a low price.

When we look at the dimensions of the board, the height of the transformer is 18.25mm and its stand to mount it into PCB has a thickness of 2mm, where the highest component on the top layer becomes 20.25mm. In the bottom layer, the highest material is the output diode, whose thickness is 3.2mm, and the board itself is 1.6mm, which means the total z-axis length of the board becomes 23.05mm. In 2D design, the x-axis and y-axis dimensions are stated, overall the board has dimensions of **54.6mm x 33mm x 23.05mm**. The volume of the design becomes **41531.49 mm³**. To have a safe, reliable, and industrial design, we have designed a box for our board in KeyCreator. While designing the box, we have added some margins to fit the board easily into the box, **where the box dimensions are 64mm x 40mm x 30mm and the box volume is 76800 mm³**. The box has screw holes for fiducial connections, and in output diodes projection, there are 6 openings that have been left, to have airflow into the box to decrease ambient temperature. The box has a cover with Metric-1.5 screw holes. The designed box and descriptions can be seen in Figures 57, 58, 59, 60, and 61.

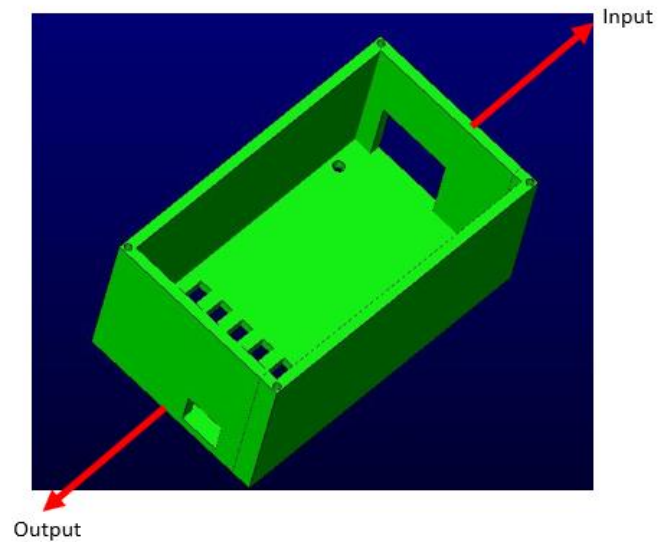


Figure 57 Top View of Board Box

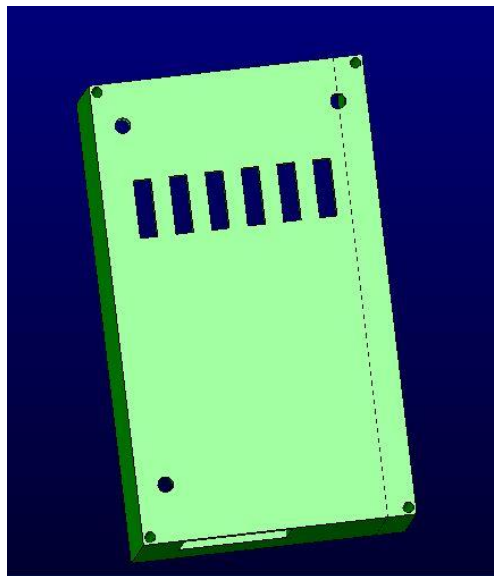


Figure 58 Bottom View of Board Box

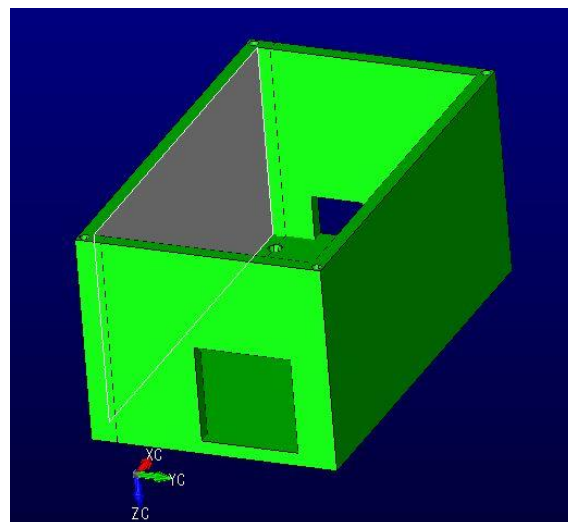


Figure 59 Input View of Board Box

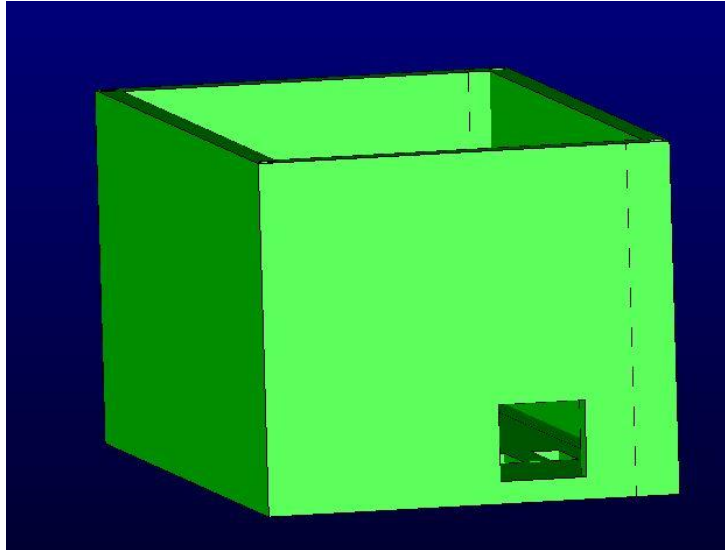


Figure 60 Output View of Board Box

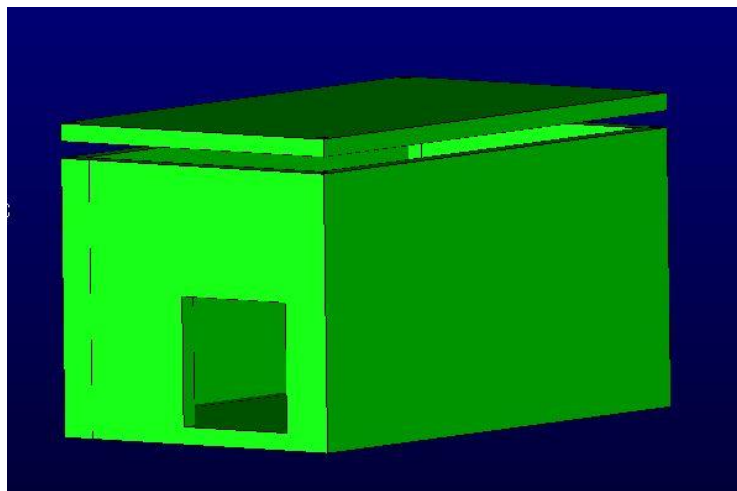


Figure 61 Board Box with Cover

To sum up, in the Hardware Design section, we have first mentioned the Schematic Design and Cost Analysis, which were very similar to Simulation Report, except for some changed components. Then, we have mentioned PCB Design by explaining rules, validations, 2D Design, 3D Design, selected PCB material, and dimensions in detail. Lastly, we have explained the box that we have designed, which has been designed to have an industrial product.

11. Cost Analysis

In Simulation Report, the total component cost was nearly \$10.78 for one board, and with consumables, we were expecting a total cost of \$12. After the simulation report, by changing some components we have decreased the component cost to \$9.78. However, when we make our transformer calculations with Litz wire, and when we added PCB cost, the total cost for one board is nearly \$13.88, and which is a quite fair price for that kind of design. Cost details can be seen in Table 5.

Table 5 Cost Analysis

Manufacturer Part Number	Description	Unit Price (\$)	Extended Price (\$)
CL31B475KOHNNNE	CAP CER 4.7UF 16V X7R 1206	0.05220	104,39
0603N470J101CT	CAP CER 47PF 100V COG/NPO 0603	0.01281	25,62
A750KK337M1CAAE014	CAP ALUM POLY 330UF 20% 16V T/H	0.18676	747,04
885012206046	CAP CER 0.1UF 16V X7R 0603	0.02400	24
C1210C104KCRCTU	CAP CER 0.1UF 500V X7R 1210	0.12644	126,44
CGA9P4X7T2W105K250KA	CAP CER 1UF 450V X7T 2220	1.39040	1390,4
C1206C104K2REC7800	CAP CER 1206 0.1UF 200V X7R	0.06401	64,01
282858-2	TERM BLK 2P SIDE ENTRY 10MM PCB	0.62589	625,89
691103110002	TERM BLK 2POS SIDE ENT 3.5MM PCB	0.53800	538
ES1CHE3_A/H	DIODE GEN PURP 150V 1A DO214AC	0.17160	171,6
S1J-E3/61T	DIODE GEN PURP 600V 1A DO214AC	0.09694	96,94
CDBB3150-HF	DIODE SCHOTTKY 150V 3A DO214AA	0.16470	494,11
CDBB3150-HF	DIODE SCHOTTKY 150V 3A DO214AA	0.18064	361,28
LT8316EFE#PBF	600VIN MICROPOWER, ISOLATED NO-O	3.10500	3105
IPD50R500CEAUMA1	MOSFET N-CH 550V 7.6A TO252	0.40554	405,54
RT1206BRD0750KL	RES SMD 50K OHM 0.1% 1/4W 1206	0.11034	110,34
RC1206FR-07499KL	RES SMD 499K OHM 1% 1/4W 1206	0.01174	35,23
ESR03EZPJ912	RES SMD 9.1K OHM 5% 1/4W 0603	0.01392	13,92
SFR03EZPJ103	RES 10 KOHM 5% 1/10W 0603	0.01493	29,86
CRCW0603121KFKEAC	RES 121K OHM 1% 1/10W 0603	0.00652	6,52
CRCW060347K0FKEAC	RES 47K OHM 1% 1/10W 0603	0.00652	6,52
CRCW08055K00JNTA	RES SMD 5K OHM 5% 1/8W 0805	0.02049	20,49
ERJ-3EKF1502V	RES SMD 15K OHM 1% 1/10W 0603	0.00677	6,77
CFG0612-FX-R010ELF	RES 0.01 OHM 1% 1W 1206	0.06400	64
RNCP0603FTD20R0	RES 20 OHM 1% 1/8W 0603	0.01060	10,6
RMCF0603FT5K60	RES 5.6K OHM 1% 1/10W 0603	0.00305	3,05
PC47EI25-Z	EI CORE SMPS TRANSFORMER 1 SET	1.02213	1022,13
SMBJE400CA	TVS DIODE 400VWM 648VC SMB	0.17017	170,17
Total Component Cost			9779,86
PCB Price			197
Litz Wire	1500 Strands-AWG38 (733000 needed)	7.99	3907,11
Total Price			13883,97

12. Conclusion

In this project, the topology selection is made considering the specs of the project. While analytical calculations and simulations were made as to the first step after topology selection, controllers which has suitable features for the project are investigated. However, there was limited controller choice due to project specs. Since the selected controller operates at variable frequencies, the project design has been made based on controller features. After the iterative transformer design that covers a small volume and meets the needs of the project, LTspice was used with the controller block in detailed simulations. Due to the controller using variable frequency, simulations were considered together with analytical calculations in both component selection and optimum design stages. It has been observed that the needs of the project have been met in the design stages made. Furthermore, power loss calculations and thermal calculations have been done and indirectly the heatsink requirement was shown. Finally, the project has been completed with a PCB design. Moreover, a suitable box to place the designed circuit was also designed.

References

- [1] <https://www.digikey.com/en/products/detail/bourns-inc/CFG0612-FX-R010ELF/9924211>
- [2] <https://www.digikey.com/en/products/detail/infineon-technologies/IPD50R500CEAUMA1/6599409>
- [3] <https://www.digikey.com/en/products/detail/stmicroelectronics/STPS30170DJF-TR/2209783>
- [4] <https://www.digikey.com/en/products/detail/stmicroelectronics/STPS1150A/1039597>
- [5] <https://www.digikey.com/en/products/detail/kemet/A750KK337M1CAAE014/6196330>
- [6] <https://www.digikey.com/en/products/detail/on-semiconductor/ES1H/1642578>
- [7] <https://www.digikey.com/en/products/detail/vishay-general-semiconductor-diodes-division/SML4764A-E3-61/3104257>
- [8] <https://www.digikey.com/en/products/detail/phoenix-contact/1714971/260639>